

DefGraspSim: Physics-based simulation of grasp outcomes for 3D deformable objects

Isabella Huang^{1,2}, Yashraj Narang², Clemens Eppner², Balakumar Sundaralingam², Miles Macklin²,
Ruzena Bajcsy¹, Tucker Hermans^{2,3}, Dieter Fox^{2,4}

Abstract—Robotic grasping of 3D deformable objects (e.g., fruits/vegetables, internal organs, bottles/boxes) is critical for real-world applications such as food processing, robotic surgery, and household automation. However, developing grasp strategies for such objects is uniquely challenging. Unlike rigid objects, deformable objects have infinite degrees of freedom and require field quantities (e.g., deformation, stress) to fully define their state. As these quantities are not easily accessible in the real world, we propose studying interaction with deformable objects through physics-based simulation. As such, we simulate grasps on a wide range of 3D deformable objects using a GPU-based implementation of the corotational finite element method (FEM). To facilitate future research, we open-source our simulated dataset (34 objects, $1e5$ Pa elasticity range, 6800 grasp evaluations, 1.1M grasp measurements), as well as a code repository that allows researchers to run our full FEM-based grasp evaluation pipeline on arbitrary 3D object models of their choice. Finally, we demonstrate good correspondence between grasp outcomes on simulated objects and their real counterparts.

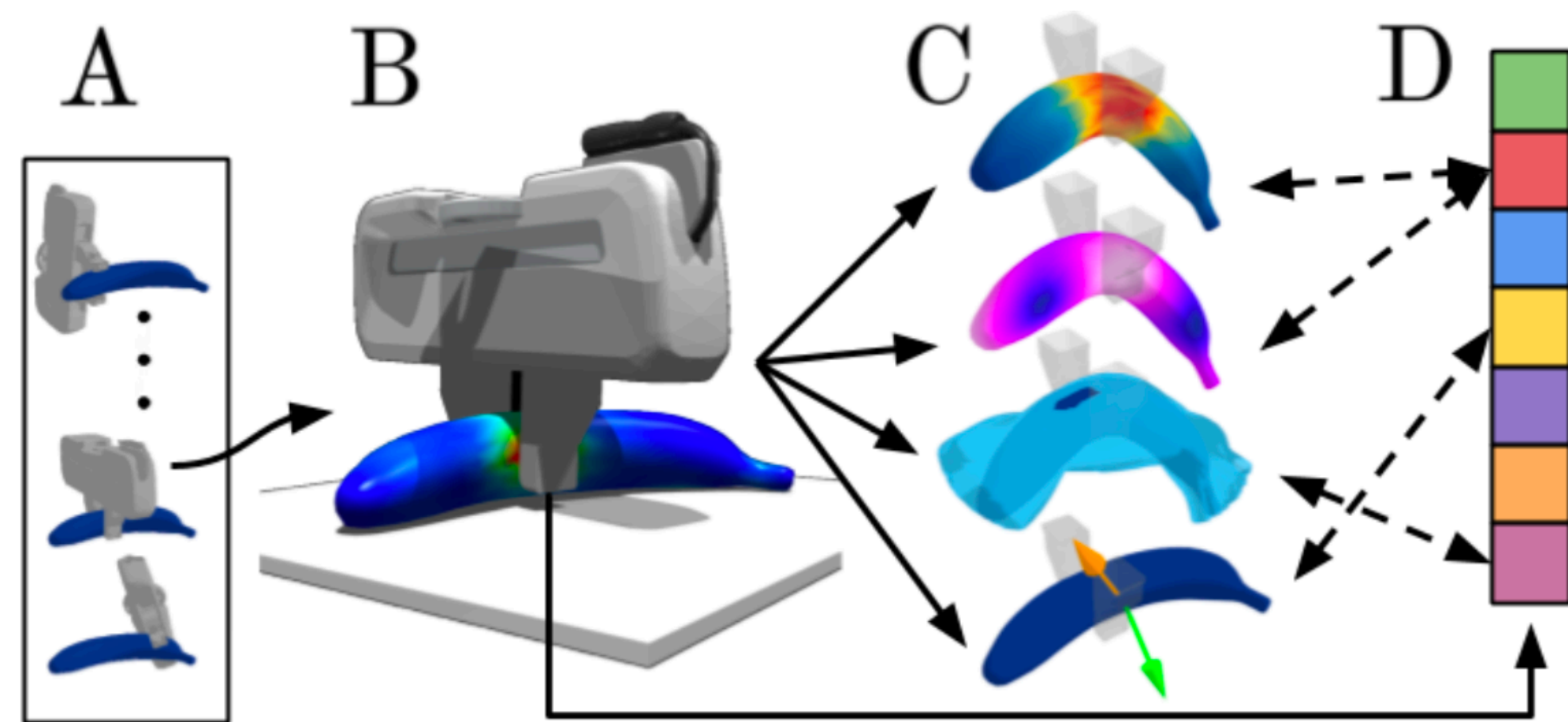
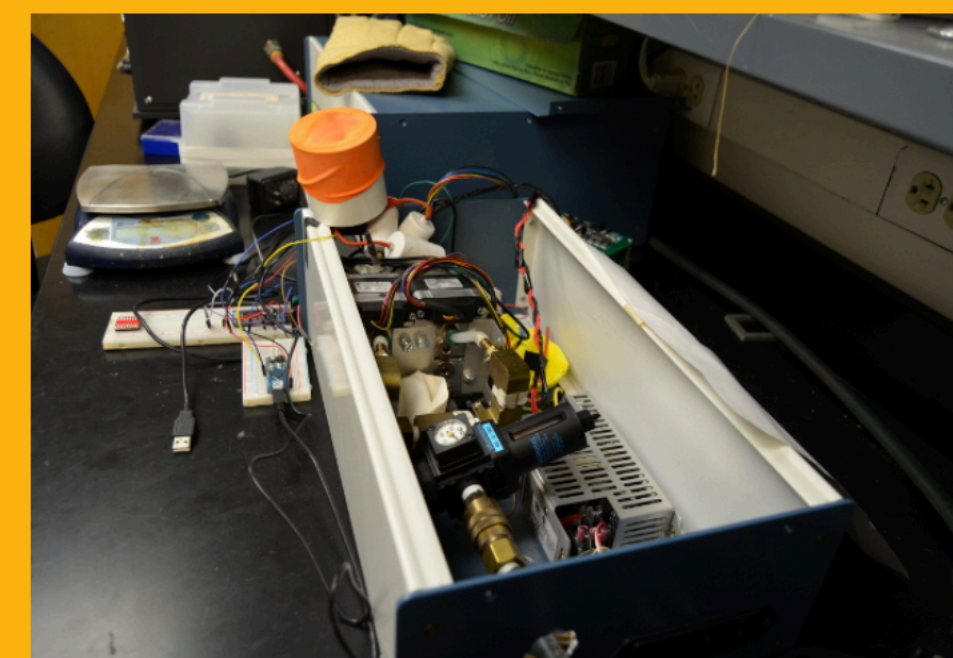
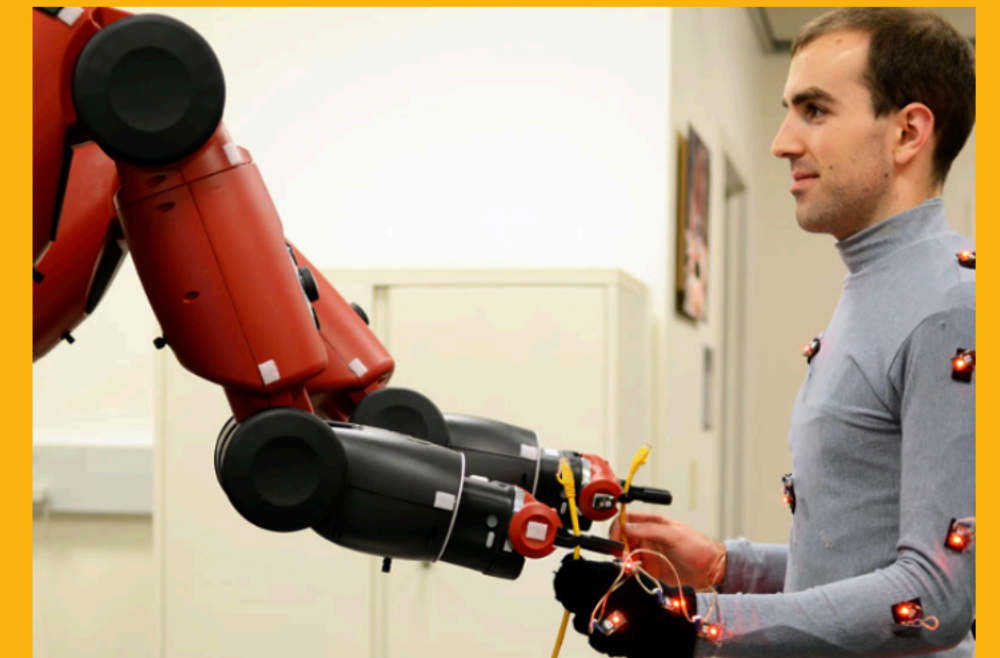
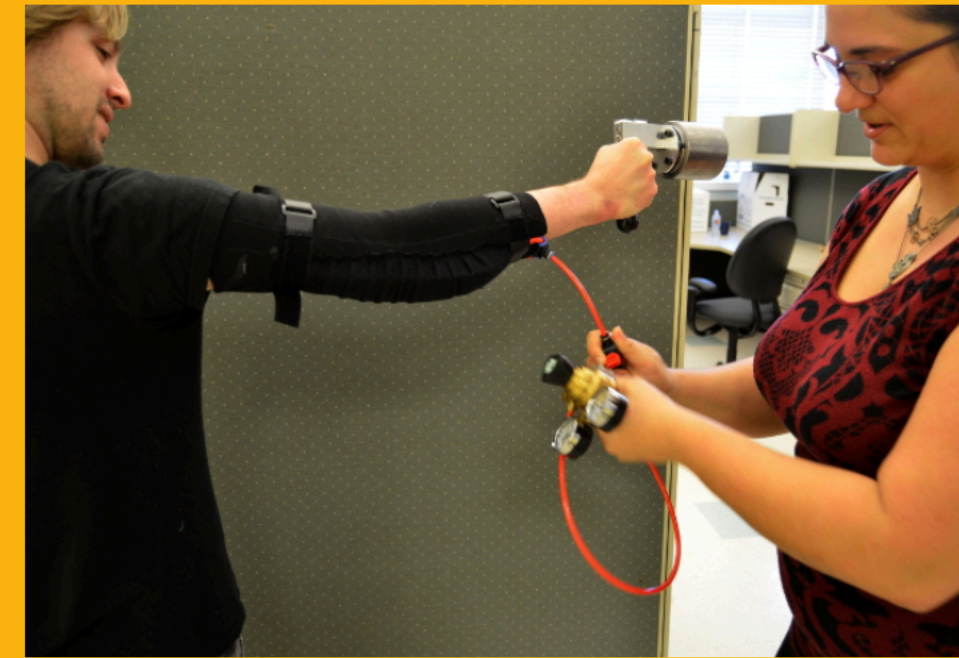


Fig. 1: (A) For a broad set of candidate grasps on a deformable object, (B) we simulate the object’s response with FEM, (C) measure performance metrics (e.g., stress, deformation, controllability, instability), and (D) identify pre-pickup grasp features that are correlated with the metrics. Our simulated dataset contains 34 objects, 6800 grasp experiments, and 1.1M unique measurements.

Welcome to the Human-Assistive Robotic Technologies Lab at UC Berkeley.



Yashraj Narang



Main Field of Interest:

Robotics

Publications

2022

DefGraspSim: Physics-Based Simulation of Grasp Outcomes on 3D Deformable Objects

Isabella Huang, [Yashraj Narang](#), [Clemens Eppner](#), [Balakumar Sundaralingam](#), Miles Macklin, Ruzena Bajcsy, [Tucker H](#)

2021

DexYCB: A Benchmark for Capturing Hand Grasping of Objects

[Yu-Wei Chao](#), [Wei Yang](#), Yu Xiang, [Pavlo Molchanov](#), [Ankur Handa](#), [Jonathan Tremblay](#), [Yashraj Narang](#), [Karl Van Wyk](#), [Ul](#)

2021

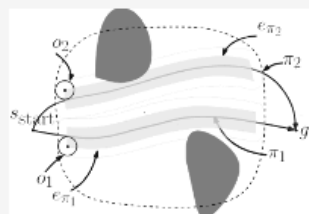


Clemens Eppner

ceppner at nvidia dot com

I am a Research Scientist in the **Seattle Robotics Lab** at **NVIDIA Research** led by **Dieter Fox**. I am interested in the problem space of grasping and manipulation, including aspects of planning, control, and perception. Although this domain may seem specific, I believe that the hybrid systems nature of grasping and manipulation is echoed in a wide range of important decision-making problems. Furthermore, I consider robotics to be a fundamentally empirical enterprise. Building systems that alter our physical world is, therefore, an integral part of my work.

Before joining NVIDIA, I received my Ph.D. at the **Robotics and Biology Lab** at TU Berlin under the supervision of **Oliver Brock**. While studying at the University of Freiburg, I wrote my Master's thesis at the **Autonomous Intelligent Systems** lab headed by **Wolfram Burgard** and worked at **Sven Behnke's Humanoid Robots Group**. I also enjoyed a research stay at **Pieter Abbeel's Robot Learning Lab** at UC Berkeley.



Alternative Paths Planner (APP) for Provably Fixed-time Manipulation Planning in Semi-structured Environments

Fahad Islam, Christopher Paxton, **Clemens Eppner**, Bryan Peele, Maxim Likhachev and Dieter Fox

Proceedings of the IEEE International Conference on Robotics and Automation (ICRA). May 2021.

[[Abstract](#)] [[BibTex](#)] [[PDF](#)]



ACRONYM: A Large-Scale Grasp Dataset Based on Simulation

Clemens Eppner, Arsalan Mousavian and Dieter Fox

Proceedings of the IEEE International Conference on Robotics and Automation (ICRA). May 2021.

[[Abstract](#)] [[BibTex](#)] [[PDF](#)] [[Data](#)] [[Code](#) ★40]



Object Rearrangement Using Learned Implicit Collision Functions

Michael Danielczuk, Arsalan Mousavian, **Clemens Eppner** and Dieter Fox

Proceedings of the IEEE International Conference on Robotics and Automation (ICRA). May 2021.

[[Abstract](#)] [[BibTex](#)] [[PDF](#)] [[Website](#)] [[Code](#) ★21]



6-DOF Grasping for Target-driven Object Manipulation in Clutter

Adithya Murali, Arsalan Mousavian, **Clemens Eppner**, Christopher Paxton and Dieter Fox

Proceedings of the IEEE International Conference on Robotics and Automation (ICRA). Paris, France. May 2020.

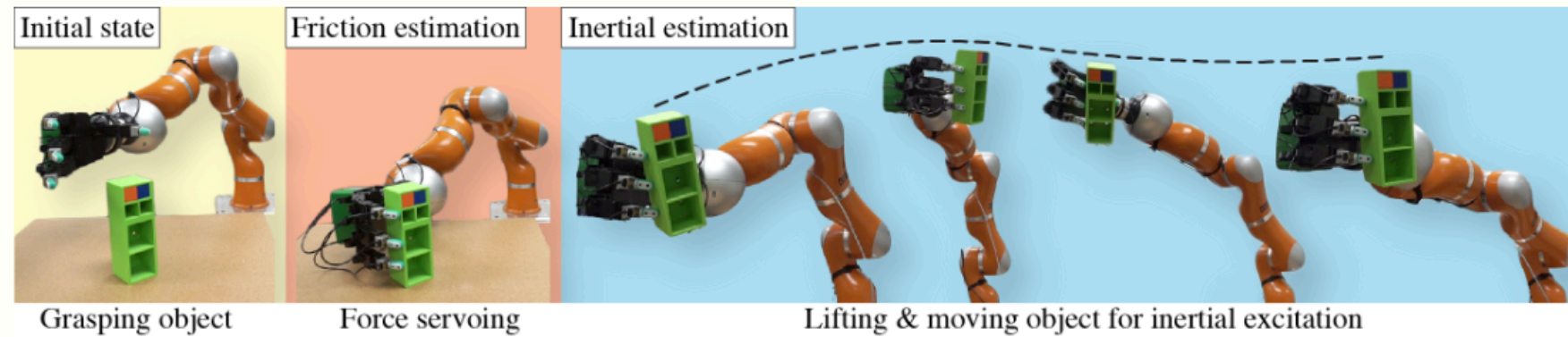
[[Abstract](#)] [[BibTex](#)] [[PDF](#)] [[Video](#)] [[Talk](#)]

[[ICRA 2020 Best Student & Best Manipulation Paper Award Finalist](#)]



Balakumar Sundaralingam

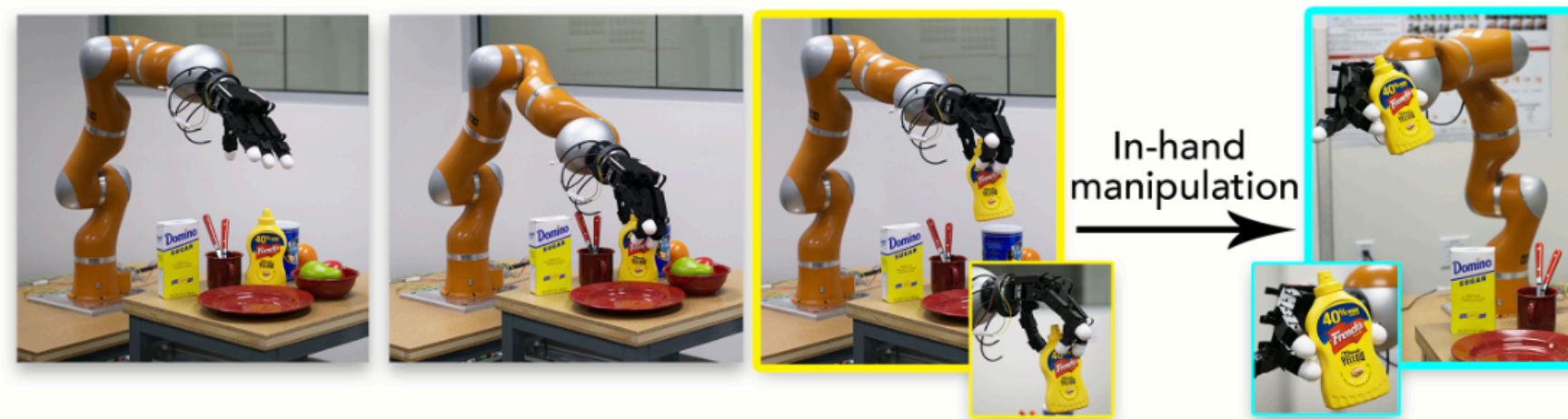
I am a Research Scientist in the **Seattle Robotics Lab** at **NVIDIA Research**. I received my **Ph.D.** in Computing (Robotics) from the University of Utah under the supervision of **Prof. Tucker Hermans**.



In-Hand Object-Dynamics Inference using Tactile Fingertips

B. Sundaralingam, T. Hermans
Preprint, 2020.

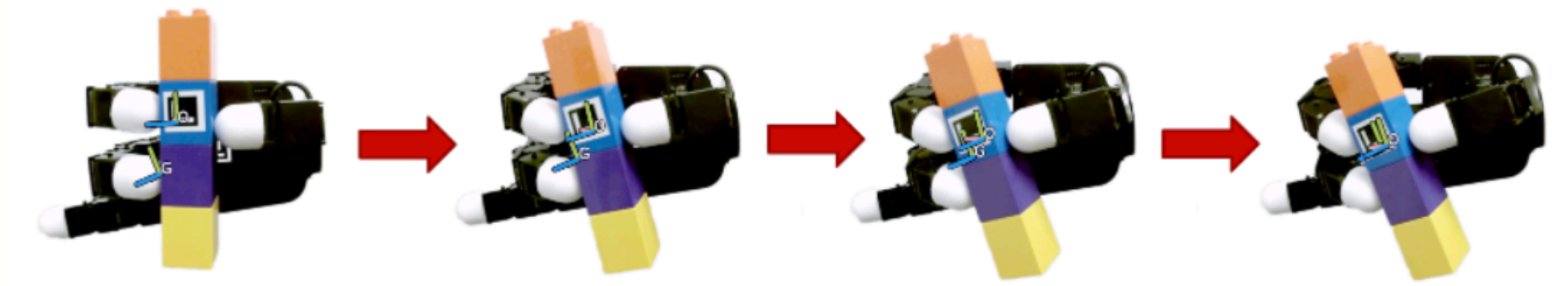
[PDF](#) [arXiv](#) [Cite](#)



Benchmarking In-Hand Manipulation

S. Cruciani*, B. Sundaralingam*, K. Hang, V. Kumar, T. Hermans, D. Kragic
RA-L, 2020.

[PDF](#) [Website](#) [arXiv](#) [Cite](#)



Relaxed-Rigidity Constraints: Kinematic Trajectory Optimization and Collision Avoidance for In-Grasp Manipulation

B. Sundaralingam, T. Hermans
Autonomous Robots, 2019.

[PDF](#) [Video](#) [Website](#) [arXiv](#) [Cite](#)



Robust Learning of Tactile Force Estimation through Robot Interaction (Best Manipulation Paper Award Finalist)

B. Sundaralingam, A. Lambert, A. Handa, B. Boots, T. Hermans, S. Birchfield, N. Ratliff, D. Fox
ICRA, 2019.

[PDF](#) [Video](#) [Website](#) [arXiv](#) [Cite](#)

Miles Macklin

Simulation and computer graphics

Blog Publications About

About

I am a Principal Engineer at NVIDIA working on physics simulation for robotics, animation, and interactive applications. I received my Ph.D. in Computer Science from the University of Copenhagen where I studied numerical methods for contact, under the supervision of Prof. Kenny Erleben. I like numerical optimization and try to design parallel methods that can leverage GPU hardware effectively. Much of my work has been integrated into products at NVIDIA including PhysX, Flex, and Isaac Gym. Before joining NVIDIA I worked in the games industry on real-time visual effects and rendering at Sony, Rocksteady, and LucasArts.

Twitter: <http://twitter.com/milesmacklin>

LinkedIn: <http://linkedin.com/in/mmacklin>

Github: <http://github.com/mmacklin>

Google Scholar: <https://scholar.google.com>



Miles Macklin @milesmacklin · Mar 22

Very happy to announce the public source release of NVIDIA Warp at #GTC22. Warp is a Python framework that makes it easy to write differentiable GPU simulation and graphics code. Code is here: github.com/NVIDIA/warp.

NVIDIA/warp

A Python framework for high performance GPU simulation and graphics



1 Contributor 4 Issues 9 Discussions 379 Stars 20 Forks

github.com
GitHub - NVIDIA/warp: A Python framework for high performance GP...



Miles Macklin · 2nd
Director, Simulation Technology at NVIDIA
3w · 🌐

This week at #GTC we released NVIDIA Warp as an open source library and extension for Omniverse. Warp aims to make it easy to write differentiable simulation and graphics code from Python. Check out the blog or the code here: <https://lnkd.in/gD3XW2XE>.



Tae Yong Kim · 2nd
NVIDIA Senior Director, Omniverse and Graphic AI
3w · 🌐



Creating Differentiable Graphics and Physics Simulation in Python with NVIDIA Warp | NVIDIA Technical Blog
developer.nvidia.com · 7 min read



- **"Predicting Stable Configurations for Semantic Placement of Novel Objects"**; Chris Paxton, Chris Xie, Tucker Hermans, Dieter Fox; *Conference on Robot Learning (CoRL)*, 2021.
- **"Parallelised Diffeomorphic Sampling-based Motion Planning"**; Tin Lai, Weiming Zhi, Tucker Hermans, Fabio Ramos; *Conference on Robot Learning (CoRL)*, 2021.
- **"Ergonomically Intelligent Physical Human-Robot Interaction: Postural Estimation, Assessment, and Optimization"**; Amir Yazdani, Roya Sabbagh Novin, Andrew Merryweather, Tucker Hermans; *AAAI Artificial Intelligence for Human-Robot Interaction Symposium (AI-HRI)*, 2021.
- **"Toward Learning Context-Dependent Tasks from Demonstration for Tendon-Driven Surgical Robots"**; Yixuan Huang, Michael Bentley, Tucker Hermans, Alan Kuntz; *International Symposium on Medical Robotics (ISMR)*, 2021.

Tucker Hermans

Associate Professor, [School of Computing](#), [University of Utah](#)

Senior Research Scientist, [NVIDIA](#)

Adjunct Associate Professor, [Department of Mechanical Engineering](#)

Member, [Utah Robotics Center](#)

- **"Planning Sensing Sequences for Subsurface 3D Tumor Mapping"**; Brian Y. Cho, Tucker Hermans, Alan Kuntz; *International Symposium on Medical Robotics (ISMR)*, 2021.
- **"Dexterous magnetic manipulation of conductive non-magnetic objects"**; Lan N. Pham, Griffin F. Tabor, Ashkan Pourkand, Jacob L. B. Aman, Tucker Hermans, Jake J. Abbott; *Nature*, 2021.
- **"In-Hand Object-Dynamics Inference using Tactile Fingertips"**; Balakumar Sundaralingam, Tucker Hermans; *IEEE Transactions on Robotics*, 2021.
- **"Optimizing Hospital Room Layout to Reduce the Risk of Patient Falls"**; Sarvenaz Chaeibakhsh, Roya Sabbagh Novin, Tucker Hermans, Andrew Merryweather, Alan Kuntz; *International Conference on Operations Research and Enterprise Systems (ICORES)*, 2021.

About Me

[[Curriculum Vitae](#)]

I'm an associate professor in the [School of Computing](#) at the [University of Utah](#), where I am affiliated with the [University of Utah Robotics Center](#) and direct the [Utah Learning Lab for Manipulation Autonomy](#).

My research focuses on autonomous learning, planning, and perception for robot manipulation. I am particularly interested in enabling robots to autonomously discover and manipulate objects with which they have no previous knowledge or experience.

Since joining Utah I have received several awards including the NSF CAREER Award in 2019, the 3M Non-Tenured Faculty Award in 2019, and a Sloan Fellowship in 2021. With my students and collaborators we have won the CoRL 2019 Best Systems Paper Award, the ICRA 2017 Best Medical Robotics Paper Award, and was finalist for the ICRA 2019 Best Manipulation Paper Award and a finalist for the Best Paper and Best Student Paper awards at ISMR 2021.

Previously I was a postdoctoral researcher in the [Intelligent Autonomous Systems lab](#) at [TU Darmstadt](#) in Darmstadt, Germany. There I worked with [Jan Peters](#) on tactile manipulation and robot learning, while serving as the team leader at TUDa for the [European Commission](#) project [TACMAN](#).

I was at [Georgia Tech](#) from 2009 to 2014 in the [School of Interactive Computing](#). There I earned my PhD in [Robotics](#) under the supervision of [Aaron Bobick](#) and [Jim Rehg](#) in the [Computational Perception Laboratory](#). My dissertation research dealt with robots learning to discover and manipulate previously unknown objects. The learning was performed on a Willow Garage [PR2 robot](#), which performed pushing tasks using visual feedback control. At Georgia Tech I also earned an MSc in Computer Science with specialization in Computational Perception and Robotics.

About me

I am a Professor in the Department of Computer Science & Engineering at the University of Washington. I grew up in Bonn, Germany, and received my Ph.D. in 1998 from the Computer Science Department at the University of Bonn. I joined the UW faculty in the fall of 2000.

I am currently sharing my time between UW and Nvidia, where I'm leading the Robotics Research Lab in Seattle. Here's some info on the [opening of that lab](#), which is located at 4545 Roosevelt Way NE.

My research interests are in robotics, artificial intelligence, and state estimation. I am the head of the UW Robotics and State Estimation Lab [RSE-Lab](#) and recently served as the academic PI of the Intel Science and Technology Center for Pervasive Computing [ISTC-PC](#). I'm a Fellow of the [AAAI](#) and [IEEE](#), recipient of the [IEEE RAS Pioneer Award](#), and served as an editor of the [IEEE Transactions on Robotics](#).



Research: The goal of my research is to enable systems to interact with people and their environment in an intelligent way. A lot of my work focuses on perception and its connection to control, where we develop techniques to extract relevant information from raw sensor data. Application areas of my work include human activity recognition, 3D mapping and tracking, and robot manipulation and control.



The Seattle landscape is getting another feature with the opening of our AI Robotics Research Lab. NVIDIA CEO Jensen Huang was there to celebrate, mixing with man and machine alike.

Leading the facility is Dieter Fox, senior director of robotics research at NVIDIA and professor at the University of Washington Paul G. Allen School of Computer Science and Engineering.

"We wanted a location that keeps us close to UW to enable easy collaboration with the university," said Fox. "For example, we often invite students from the UW robotics community to spend time here and attend seminars with external speakers."

The lab opened in November with 14 researchers and expects to triple in size by midyear, including visiting faculty and interns.



Dieter Fox, a roboticist and University of Washington professor, leads the new AI Robotics Research Lab in Seattle.

Motivation

- Robotic grasping of 3D deformable is **underexplored** relative to rope and cloth
- Yet, it is **critical** for applications such as:
 - food handling
 - surgery
 - domestic tasks

Challenge #1 of 4

Performance Metrics for Deformable Object Grasping

Classical analytical **metrics** for grasping rigid objects do not typically consider deformation.

Grasp success is affected by compliance

- e.g., grasping a stuffed toy haphazardly is ok
- e.g., grasping a rigid container haphazardly can lead to crushing

Proposed solution —> introduce **7 performance metrics** suitable for deformable objects

Challenge #2 of 4

Observable Features for Deformable Object Grasping

Many obvious performance metrics such as volumetric stress and strain may be **unobservable**.

Real world grasping requires estimators that can operate on observable quantities.

Proposed solution —> introduce **7 grasp features** which may be able to predict performance metrics for deformable objects

Challenge #3 of 4

Lack of Evaluation Framework, Dataset, or Codebase

There is no existing **benchmark, dataset, or codebase** for the task of evaluating grasps of 3D deformable objects.

Proposed solution —> release **DefGraspSim** for FEM-based grasp evaluations on arbitrary 3D objects

Proposed solution —> release **dataset** of results from testing with this system

- 34 objects
- 6800 grasp evaluations
- 1.1M measurements

Challenge #4 of 4

Sim2Real

Simulations do not always match reality.

Proposed solution —> perform pilot sim2real study showing promising correspondence.

Summary of Contributions

Performance metrics

Observable grasp features

Codebase and dataset from many example grasps of deformable objects

Sim2real tests

Related Work 1 of 2

Rigid object grasp planning

- Model-based approaches

- Data-driven approaches

Rigid body grasp simulators (e.g., Graspl! and OpenGRASP)

Deformable object simulators

- Kelvin-Voigt elements

- mass-spring models

- 2D FEM models

- 3D FEM (gold standard)

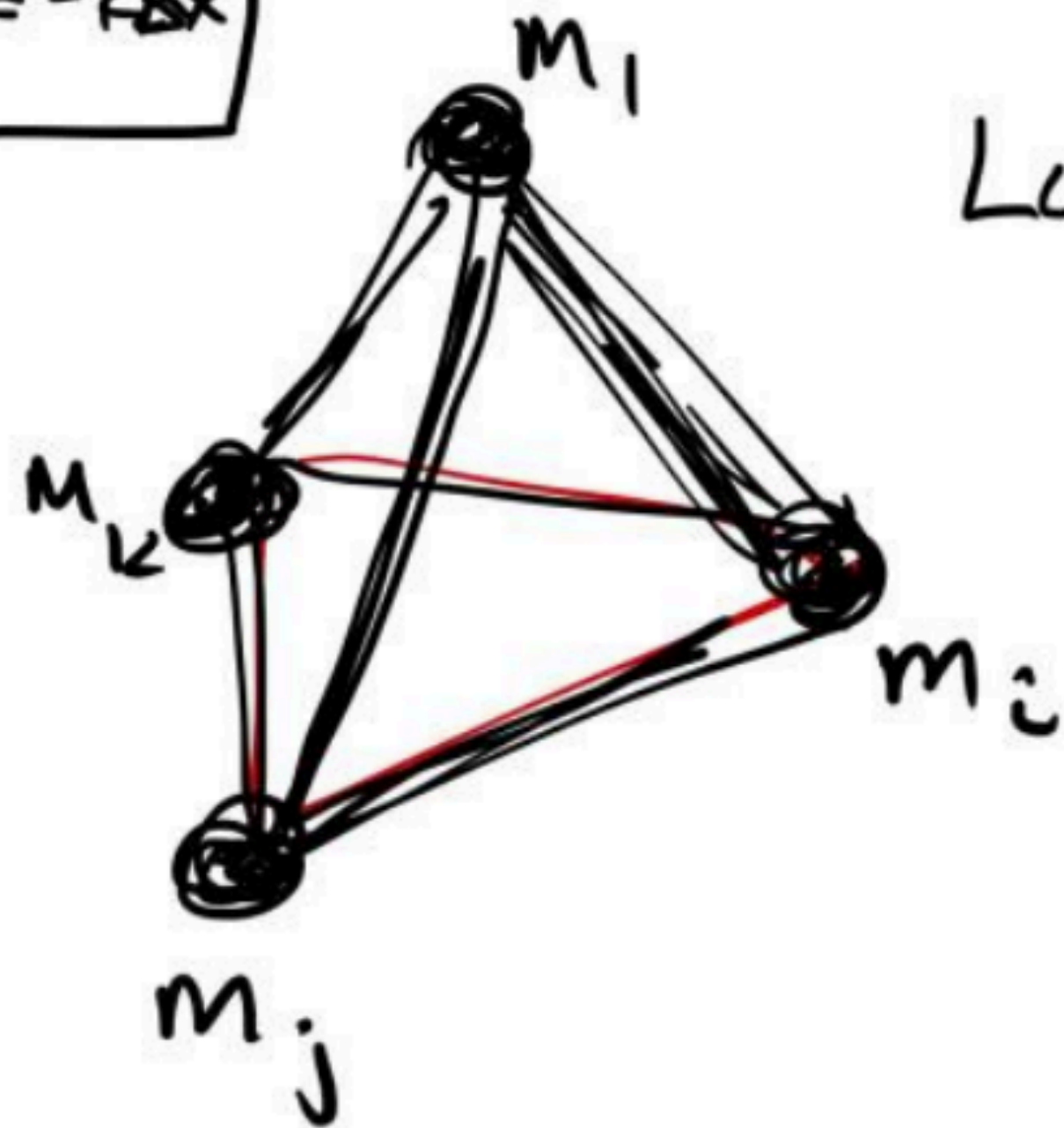
Many existing 3D FEM simulators do not offer good support for robotic control (e.g., built-in joint control)

TABLE I: Comparisons between Isaac Gym and other robotics simulators that support both 3D deformable bodies and actuator interactions.

Simulator	Interactions	3D geometries	Materials	Underlying model	Observable states	Processor
MuJoCo [4]	soft-rigid, rigid-rigid	Boxes, cylinders, ellipsoids	Homogeneous isotropic elastic	Mass-spring with sur- face nodes	Nodal positions	CPU
PyBullet 3 [5]	soft-rigid, soft-soft, rigid-rigid	Arbitrary geome- tries	Homogeneous isotropic elas- tic/hyperelastic	Mass-spring or Neo- Hookean volumetric FEM	Nodal positions, contact points & forces	CPU
IPC-GraspSim [6]	soft-soft	Arbitrary geome- tries	Homogeneous isotropic elastic	Incremental potential contact model	Nodal positions, velocities, and ac- celerations	CPU
Isaac Gym [7]	soft-rigid, rigid-rigid	Arbitrary geome- tries	Homogeneous isotropic elastic	Co-rotational linear volumetric FEM	Nodal positions & velocities, con- tact points & forces, element stress tensors	GPU

Choice: GPU-accelerated Isaac Gym simulator

$$f = -kx$$



Lumped
mass
model

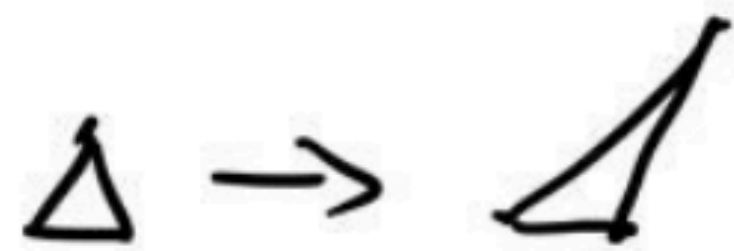
FINITE ELEMENT SIMULATION

(1) Compute Strain (deformation)

Green's strain tensor ϵ

3x3 Matrix

Strain rate tensor ν



(2) Compute Stress (internal force)

3x3 matrix (tensor) $\sigma^{(\epsilon)}$

elastic stress due to strain $\sigma^{(\epsilon)}$

viscous stress due to strain rate $\sigma^{(\nu)}$

Simplifying assumption — isotropic material

4 parameters
that determine
behavior

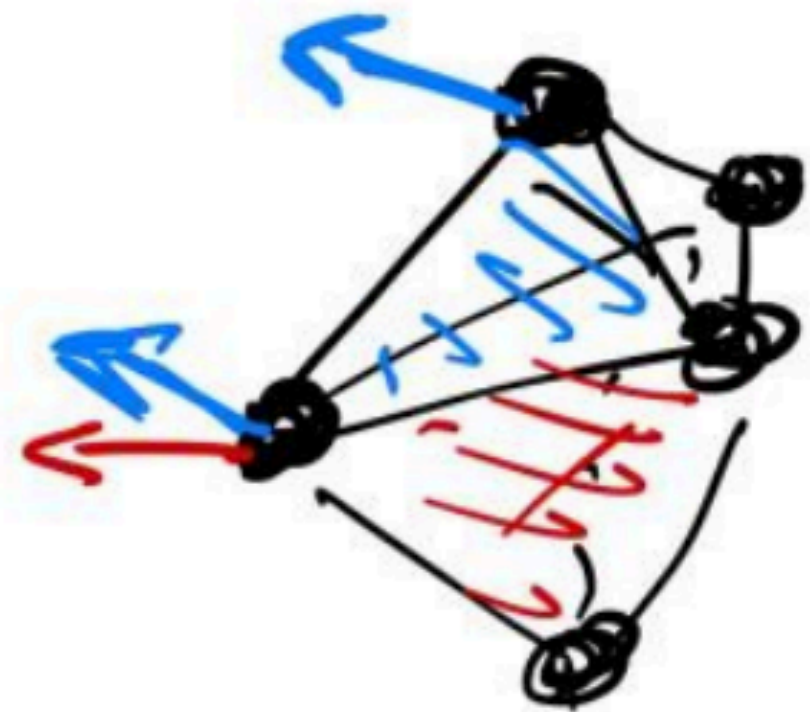
μ - rigidity

λ - resist Δ volume

ϕ, ψ

- how quickly dissipates
kinetic energy

(3) Compute node forces from stress



(4) Update node state
from forces

Some definitions.....

Neo-Hookean

A neo-Hookean solid[1] [2] is a hyperelastic material model, similar to Hooke's law, that can be used for predicting the nonlinear stress-strain behavior of materials undergoing large deformations. In contrast to linear elastic materials, the stress-strain curve of a neo-Hookean material is not linear. Instead, the relationship between applied stress and strain is initially linear, but at a certain point the stress-strain curve will plateau. The neo-Hookean model does not account for the dissipative release of energy as heat while straining the material and perfect elasticity is assumed at all stages of deformation.

The neo-Hookean model is based on the statistical thermodynamics of cross-linked polymer chains and is usable for plastics and rubber-like substances ... and is typically accurate only for strains less than 20%

Invertible Finite Elements For Robust Simulation of Large Deformation

G. Irving[†], J. Teran[‡], and R. Fedkiw[§]

Stanford University

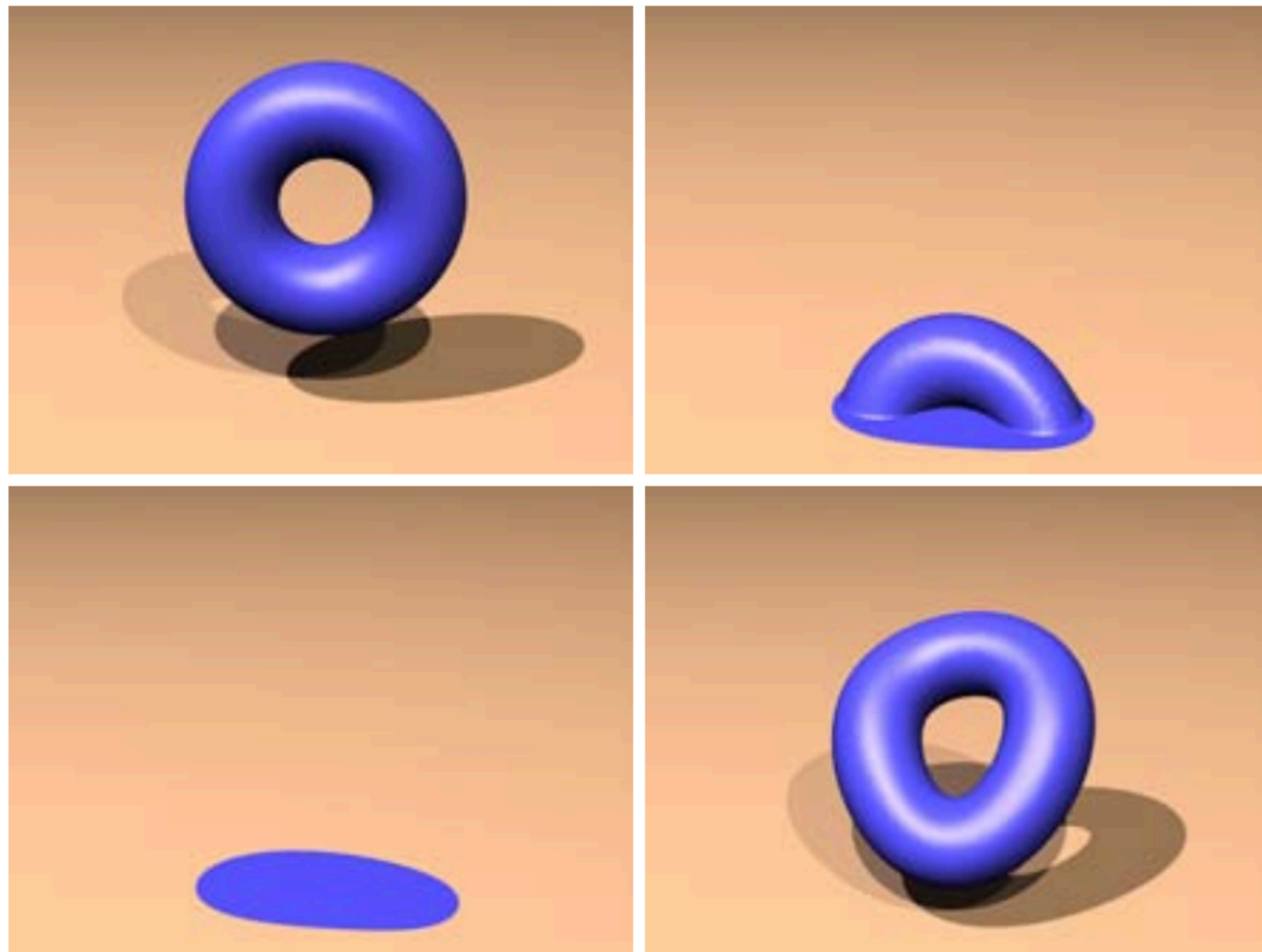


Figure 2: A torus with zero strength collapses into a puddle. When the strength is increased, the torus recovers.

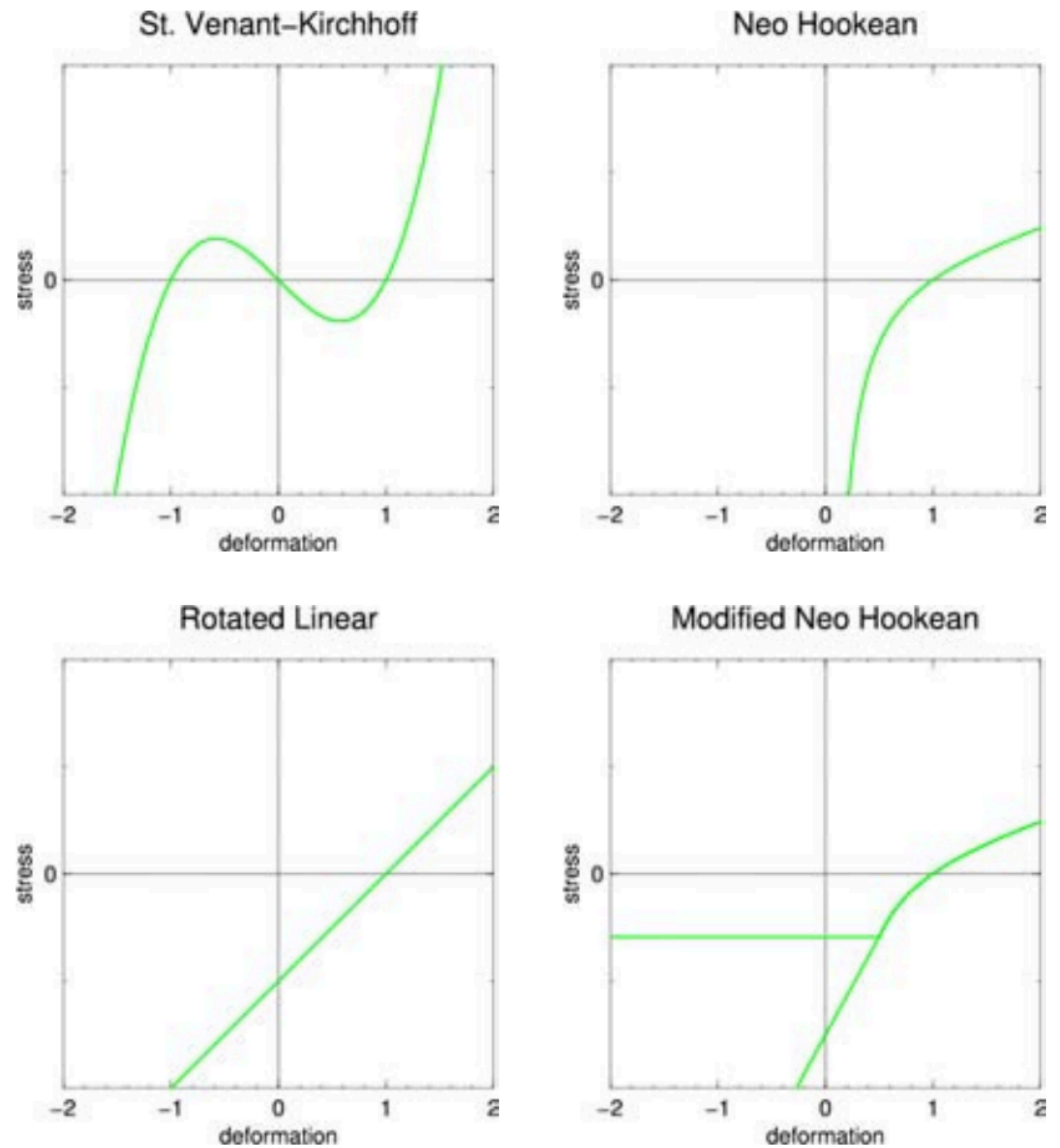


Figure 3: The relationship between the first Piola-Kirchhoff stress $\hat{\mathbf{P}}$ and the deformation gradient $\hat{\mathbf{F}}$ for various constitutive models.

Stable Neo-Hookean Flesh Simulation

BREANNAN SMITH, FERNANDO DE GOES, and THEODORE KIM, Pixar Animation Studios



Fig. 1. **Left:** Thirteen skeletal bones drive a hexahedral lattice with 45,809 elements and 156,078 degrees of freedom. **Center:** A quasi-static simulation with our new Neo-Hookean model and a Poisson's ratio of $\nu = 0.488$. Wrinkles and bulges emerge from our model's excellent volume-preserving properties. An average time step with our model took 13.7 Newton iterations, 5,860 Conjugate Gradient (CG) iterations, and 25.6 seconds. **Right:** The same simulation with corotational elasticity and $\nu = 0.488$. The model fails to preserve volume and instead collapses the trapezius and forms a spurious fold around the shoulder blade. The artifacts persist across all values of ν . An average time step with this model took 17.9 Newton iterations, 16,183 CG iterations, and 46.6 seconds. ©Disney/Pixar.

Some definitions.....

CoRotational FEM

The corotational method solves nonlinear structural problems by splitting the deformation of beam elements into rigid body motions and local deformations. In contrast to linear FE that assumes small rotations, large rotations are captured, in the corotational approach, by rigid body rotation matrices. Linear beam elements can, therefore, be used as long as strains remain small within each element

High fidelity simulation of corotational linear FEM for incompressible materials

Mihai Frâncu
University of Copenhagen

Arni Asgeirsson
University of Copenhagen

Kenny Erleben
University of Copenhagen

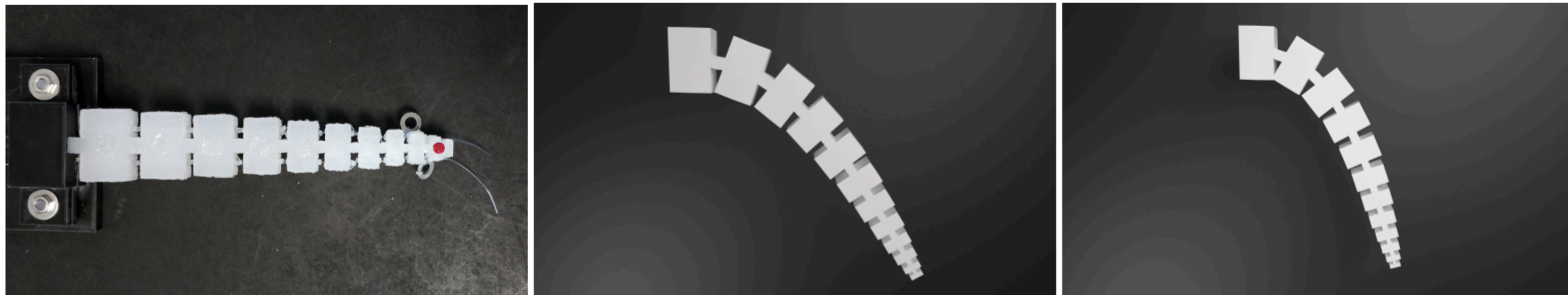


Figure 1: Soft robot made out of silicone rubber. Left: real life soft robot. Middle: the soft robot hanging under gravity simulated using corotational FEM. Right: the same simulation using our method. The corotational method suffers from locking, while our method has a wider range of motion using the same linear mesh. Elastic parameters: $E=262$ kPa, $\nu=0.49$.

ABSTRACT

We present a novel method of simulating incompressible materials undergoing large deformation without locking artifacts. We apply it for simulating silicone soft robots with a Poisson ratio close to 0.5. The new approach is based on the mixed finite element method (FEM) using a pressure-displacement formulation; the deviatoric deformation is still handled in a traditional fashion. We support large deformations without volume increase using the corotational formulation of linear elasticity. Stability is ensured by an implicit integration scheme which always reduces to a sparse linear system. For even more deformation accuracy we support higher order simulation through the use of Bernstein-Bézier polynomials.

1 INTRODUCTION

Incompressible materials form an important class of materials that has been seeing increased interest in the simulation community. In computer graphics the focus is on simulating realistic skin deformation. Other applications include biomedical ones and soft robotics. We are particularly interested in simulating and actuating such soft robots made out of silicone rubber.

Training deep neural networks for data-driven control policies in robotics requires simulations to be used a great number of times [Chebotar et al. 2018]. Therefore, the simulation has to be fast while still being as highly accurate as possible so the gap between simulation and reality is not too wide. We call these constraints the *high fidelity* requirement.

TABLE I: Comparisons between Isaac Gym and other robotics simulators that support both 3D deformable bodies and actuator interactions.

Simulator	Interactions	3D geometries	Materials	Underlying model	Observable states	Processor
MuJoCo [4]	soft-rigid, rigid-rigid	Boxes, cylinders, ellipsoids	Homogeneous isotropic elastic	Mass-spring with sur- face nodes	Nodal positions	CPU
PyBullet 3 [5]	soft-rigid, soft-soft, rigid-rigid	Arbitrary geome- tries	Homogeneous isotropic elas- tic/hyperelastic	Mass-spring or Neo- Hookean volumetric FEM	Nodal positions, contact points & forces	CPU
IPC-GraspSim [6]	soft-soft	Arbitrary geome- tries	Homogeneous isotropic elastic	Incremental potential contact model	Nodal positions, velocities, and ac- celerations	CPU
Isaac Gym [7]	soft-rigid, rigid-rigid	Arbitrary geome- tries	Homogeneous isotropic elastic	Co-rotational linear volumetric FEM	Nodal positions & velocities, con- tact points & forces, element stress tensors	GPU

Choice: GPU-accelerated Isaac Gym simulator

Related Work 2 of 2

Performance metrics on deformable objects

- pickup success
- strain energy (e.g., Ken Goldberg's deform closure metric for 2D grasps quantifies the work required to extract a grasped object)
- deformation
- stress

Grasp features on rigid objects

- force and form closure
- grasp polygon area

Grasp features on deformable objects

- Ken Goldberg and colleagues study the work performed on containers during grasping to predict whether liquid contents would be displaced

Overview

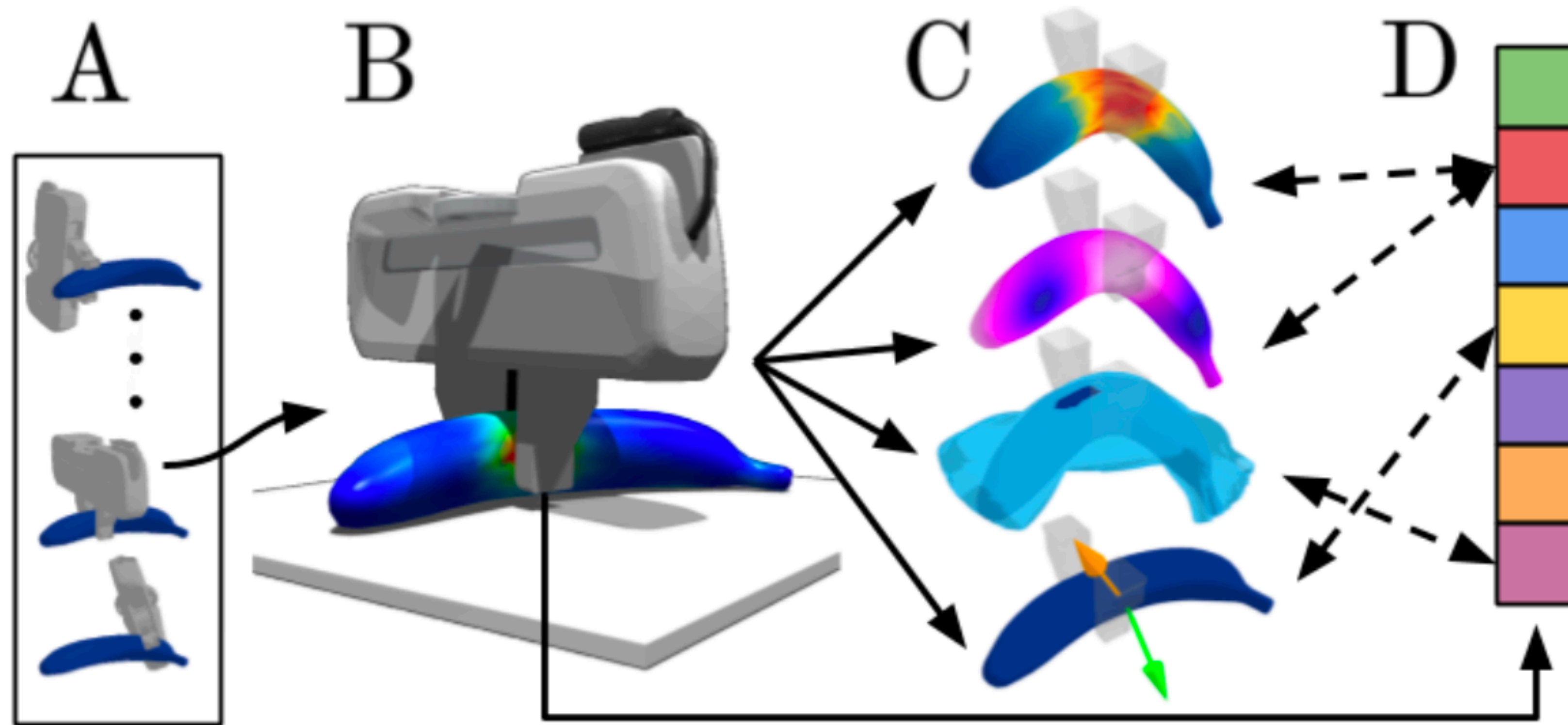


Fig. 1: (A) For a broad set of candidate grasps on a deformable object, (B) we simulate the object's response with FEM, (C) measure performance metrics (e.g., stress, deformation, controllability, instability), and (D) identify pre-pickup grasp features that are correlated with the metrics. Our simulated dataset contains 34 objects, 6800 grasp experiments, and $1.1M$ unique measurements.

34 Objects

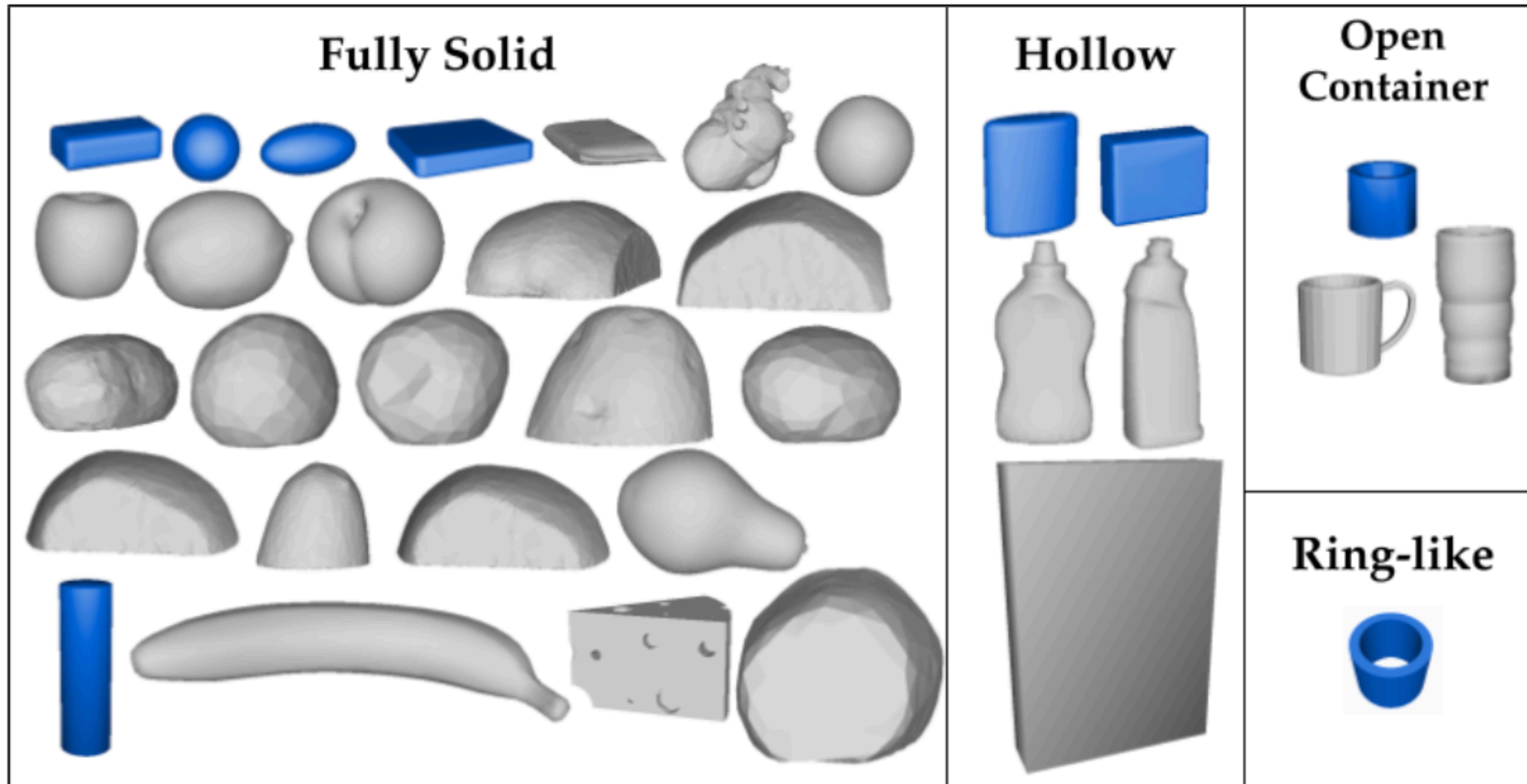


Fig. 2: The 34 evaluated objects grouped by geometry and dimension (shown to scale). Objects in blue are self-designed primitives; those in gray are scaled models from open datasets [39], [40], [41], [42].

Range of Stiffnesses

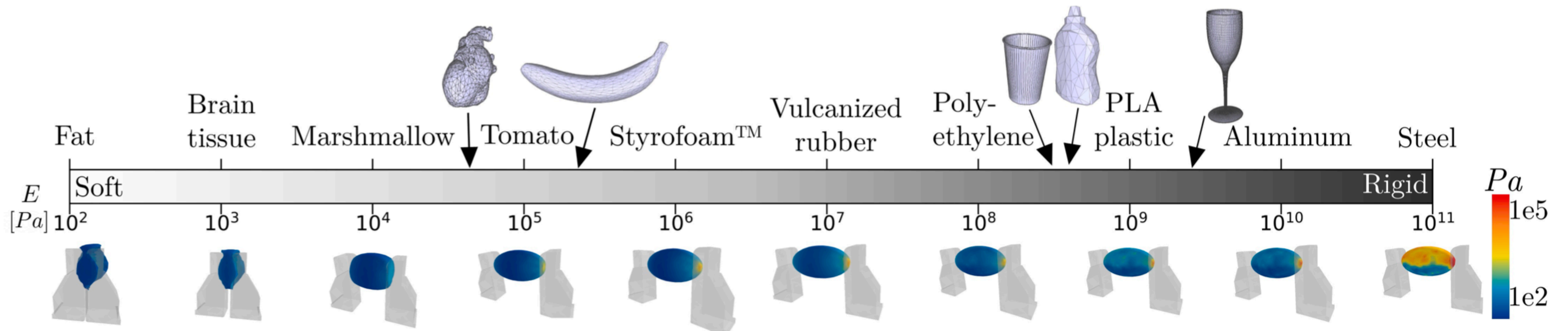


Fig. 3: Young's modulus E for various materials (adapted from [43]). (Top): real-world objects and their typical E . (Bottom): Stress distributions of an ellipsoid under 1 N of grasp force. Soft ellipsoids undergo large deformations; rigid ones have high-stress regions.

Flow of Experiments

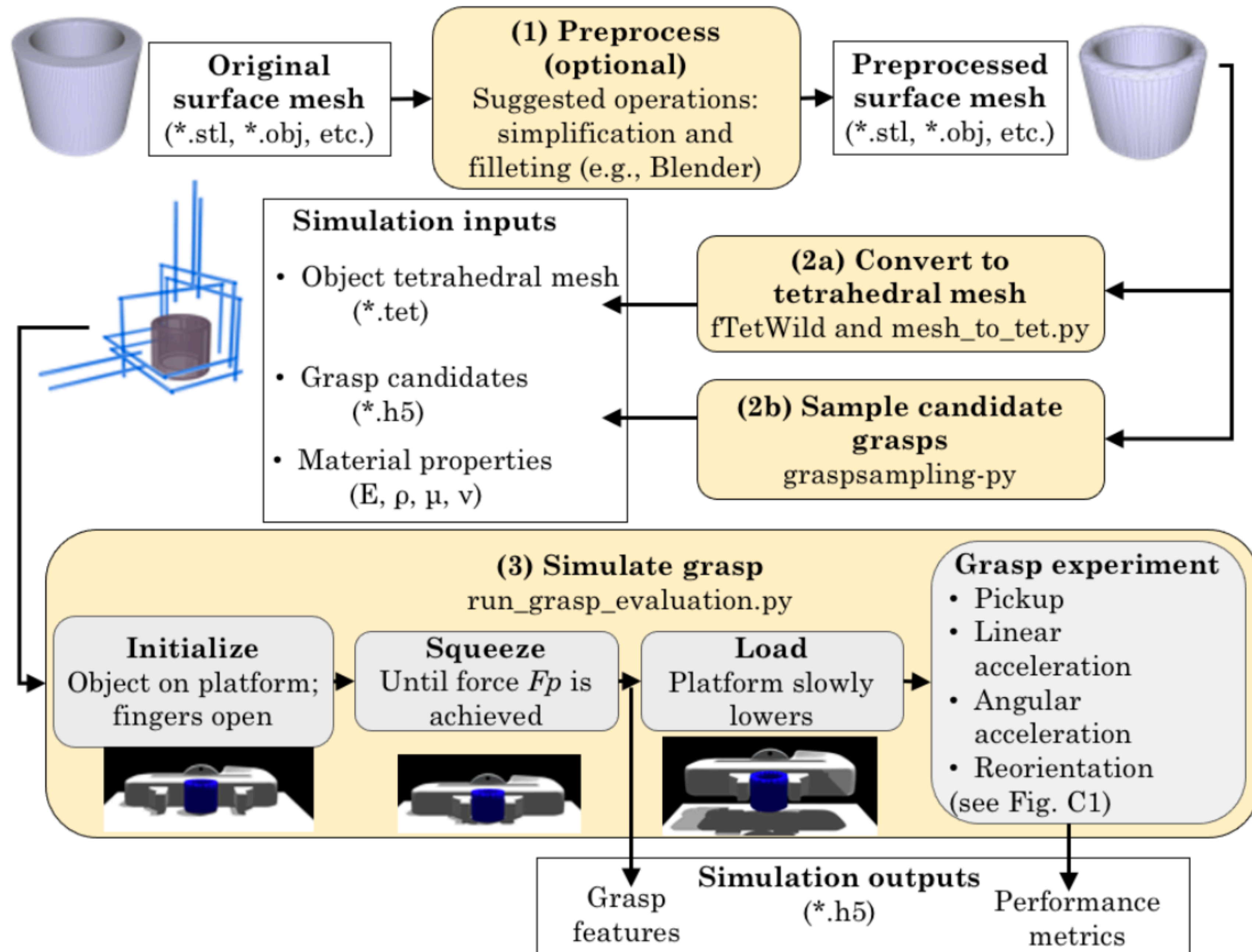
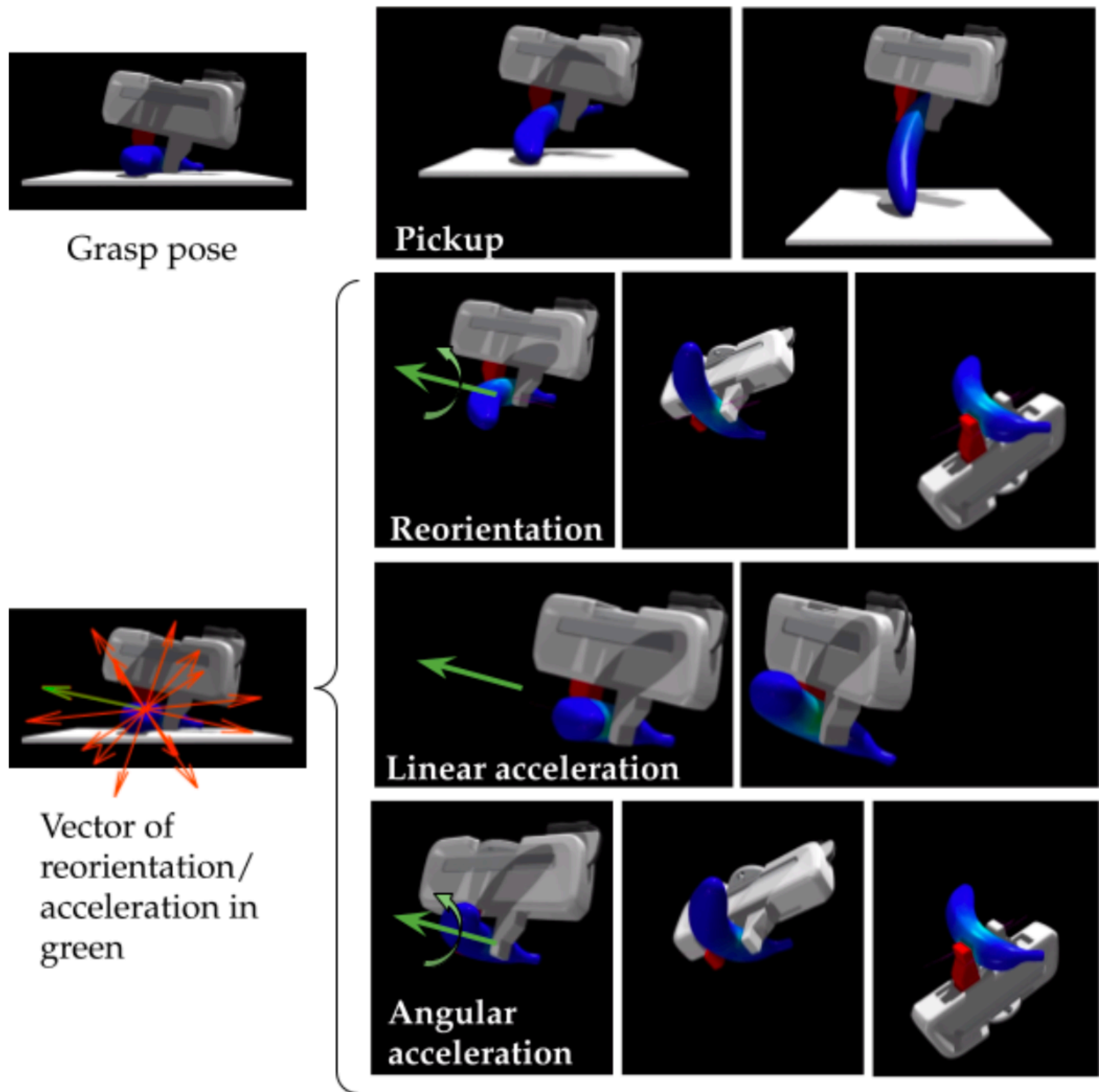


Fig. 5: Software flow diagram of the DefGraspSim codebase.



Pickup: success = maintain contact for 5 seconds

Reorientation: increase grasp force to minimum required to resist slip. 64 reorientation states. Record stress and deformation fields.

Linear/angular acceleration: 16 directions. Record acceleration at which one finger loses contact and average over all directions.

Fig. 4: Example frames from the execution of four different experiments per grasp on a banana: pickup, reorient, twist (angular acceleration), and shake (linear acceleration).

Some Details

Simulate at a frequency of 1500Hz

Simulator executes at 5-10 fps

Each grasp experiment takes 2-7 minute to run

For all experiments our objects have density $\rho = 1000 \frac{kg}{m^3}$, Poisson's ratio $\nu = 0.3$, coefficient of friction $\mu = 0.7$, and Young's modulus $E \in \mathcal{E} = \{2e4, 2e5, 2e6, 2e9\} Pa$. \mathcal{E} covers a wide range of real materials, from human skin ($\sim 10^4 Pa$) to ABS plastic ($\sim 10^9 Pa$) (Fig. 3). The target squeezing force on an object is $F_p = 1.3 \times \frac{mg}{\mu}$ (where m is mass and g is gravity), which is the force required to support the object's weight with a factor of safety. For a fixed E , increasing μ decreases F_p as well as the induced deformation. This effect is essentially the same as if μ is fixed while E is increased, since an elastically stiffer object will also deform less for the same F_p applied. Thus, we fix μ and vary E .

7 Grasp Performance Metrics

1. Pickup success.

Binary

2. Stress.

Element-wise stress field. Collect max over all elements / compare to yield threshold.

3. Deformation

Subtract out optimal rigid body transform and collect max displacement over all elements.

4. Strain energy

Elastic potential energy stored in the object

5. Linear instability

Minimum acceleration at which the object loses contact

6. Angular instability

Minimum acceleration at which the object loses contact

7. Deformation controllability

Max deformation when the object is reoriented under gravity

Minimize to obtain more rigid behavior on pickup / maximize to achieve deformation goal (e.g., insertion of endoscope)

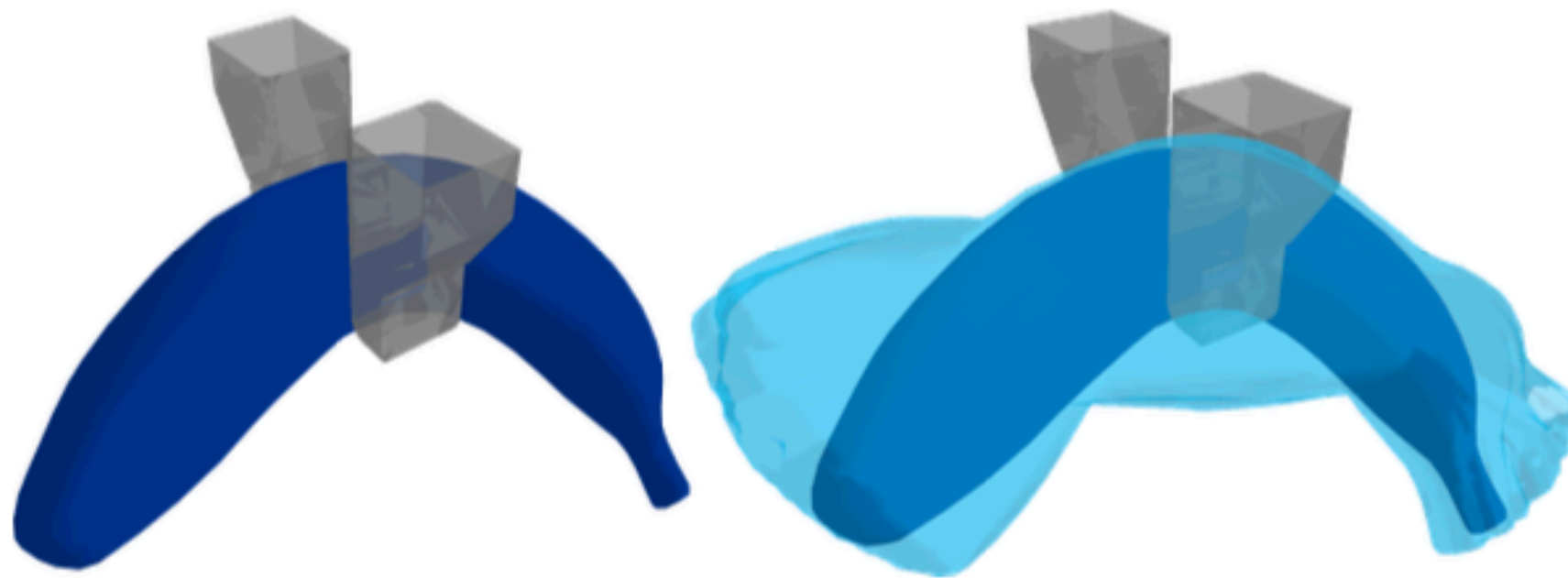


Fig. 6: Illustration of deformation controllability. A soft banana-shaped object under pickup (left); the union of all shape configurations achieved under reorientation, superimposed in light blue (right).

7 Grasp Features

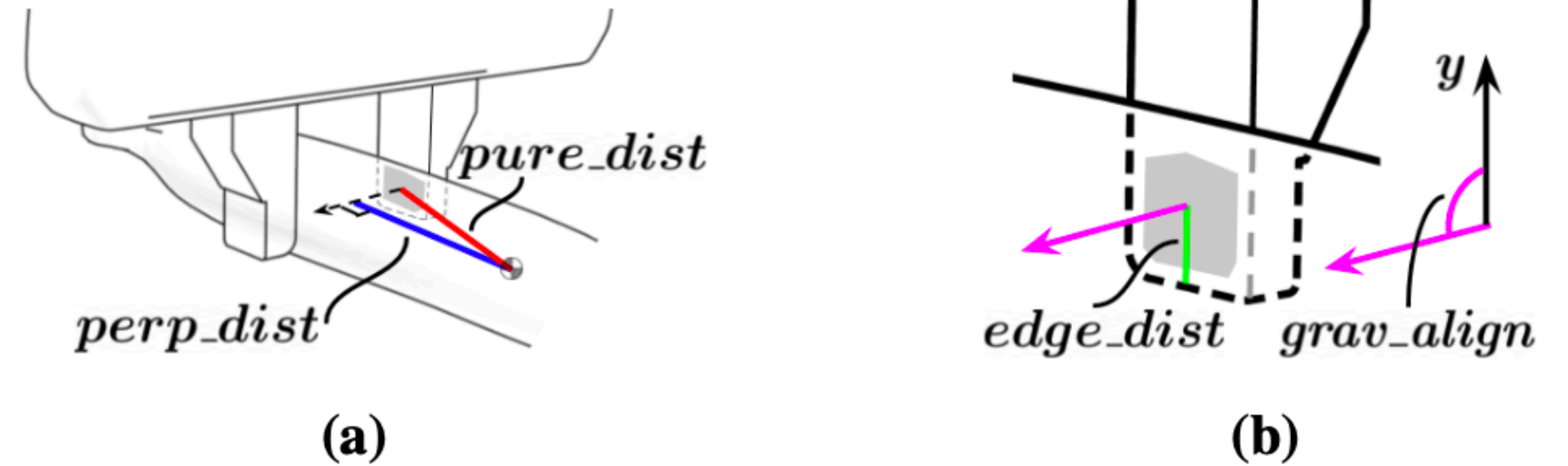


Fig. 7: Four grasp features illustrated on a Franka gripper.

TABLE II: Grasp features, their descriptive

Feature	Abbreviation	Definition and Relevance	Usage in Literature
Contact patch distance to centroid	<i>pure_dist</i>	Distance from the center of each finger's contact patch to the object's center of mass (COM) (Fig. 7a), averaged over the two fingers.	[37], [51]
Contact patch perpendicular distance to centroid	<i>perp_dist</i>	Perpendicular distance from the center of each finger's contact patch to the object's COM (Fig. 7a), averaged over the two fingers; quantifies distance from lines of action of squeezing force.	[52]
Number of contact points	<i>num_contacts</i>	Number of contact points on each finger, averaged over the fingers; quantifies amount of contact made.	[37], [51]
Contact patch distance to finger edge	<i>edge_dist</i>	Distance from each finger's distal edge to the center of its contact patch (Fig. 7b), averaged over the two fingers.	[53]
Gripper squeezing distance	<i>squeeze_dist</i>	Change in finger separation from initial contact to the point at which F_p is achieved; quantifies local deformation applied to the object.	[34]
Gripper separation	<i>gripper_sep</i>	Finger separation upon achieving F_p ; quantifies the thickness of material between the fingers at grasp.	[37]
Alignment with gravity	<i>grav_align</i>	Angle between the finger normal and the global vertical; grounds the grasp pose to a fixed frame (Fig. 7b).	[54]

Simulation tests on 5 real objects

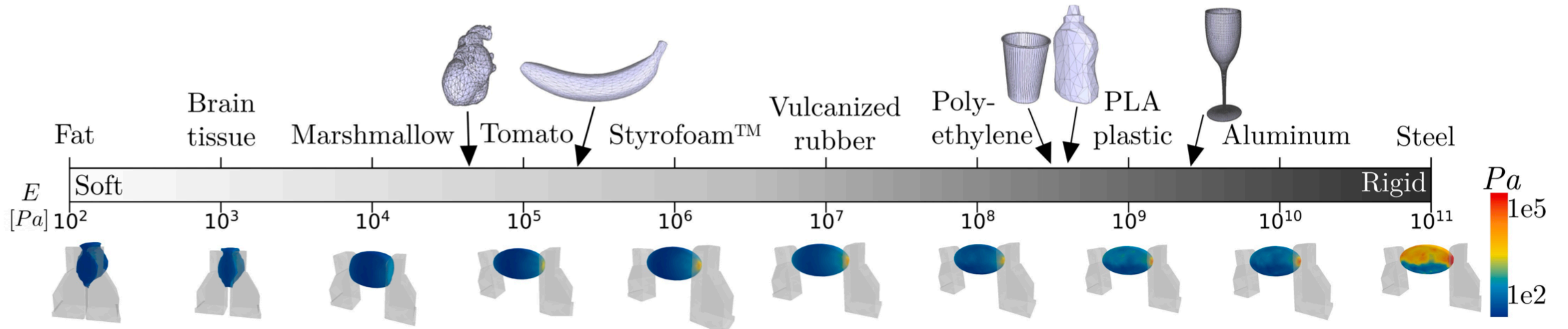
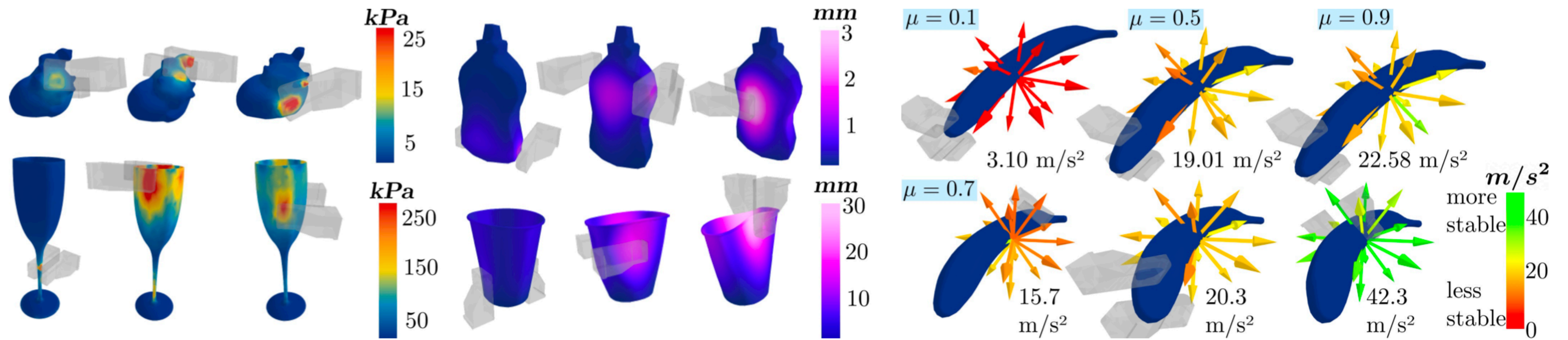


Fig. 3: Young's modulus E for various materials (adapted from [43]). (Top): real-world objects and their typical E . (Bottom): Stress distributions of an ellipsoid under 1 N of grasp force. Soft ellipsoids undergo large deformations; rigid ones have high-stress regions.

Simulation Results

Stress, deformation, and linear stability



(a) Simulated stress fields after pickup for various grasps on a (top) heart and (bottom) wine glass. Objects are colored by the von Mises stress field.

(b) Simulated deformation fields after pickup for various grasps on a (top) mustard bottle and (bottom) plastic cup. Objects are colored by the l^2 -norm of the deformation field.

(c) Linear stability of grasps on a banana at 4 N of grasp force under (top) the same grasp but variable friction μ , and (bottom) the same μ but variable grasps. Arrows are colored by the maximum acceleration in that direction before loss of contact. Number indicates the average acceleration at failure over all 16 directions.

Fig. 8: Examples of simulated grasp outcomes on 5 objects, with visualizations of (a) stress, (b) deformation, and (c) linear stability.

Sim2Real Tofu

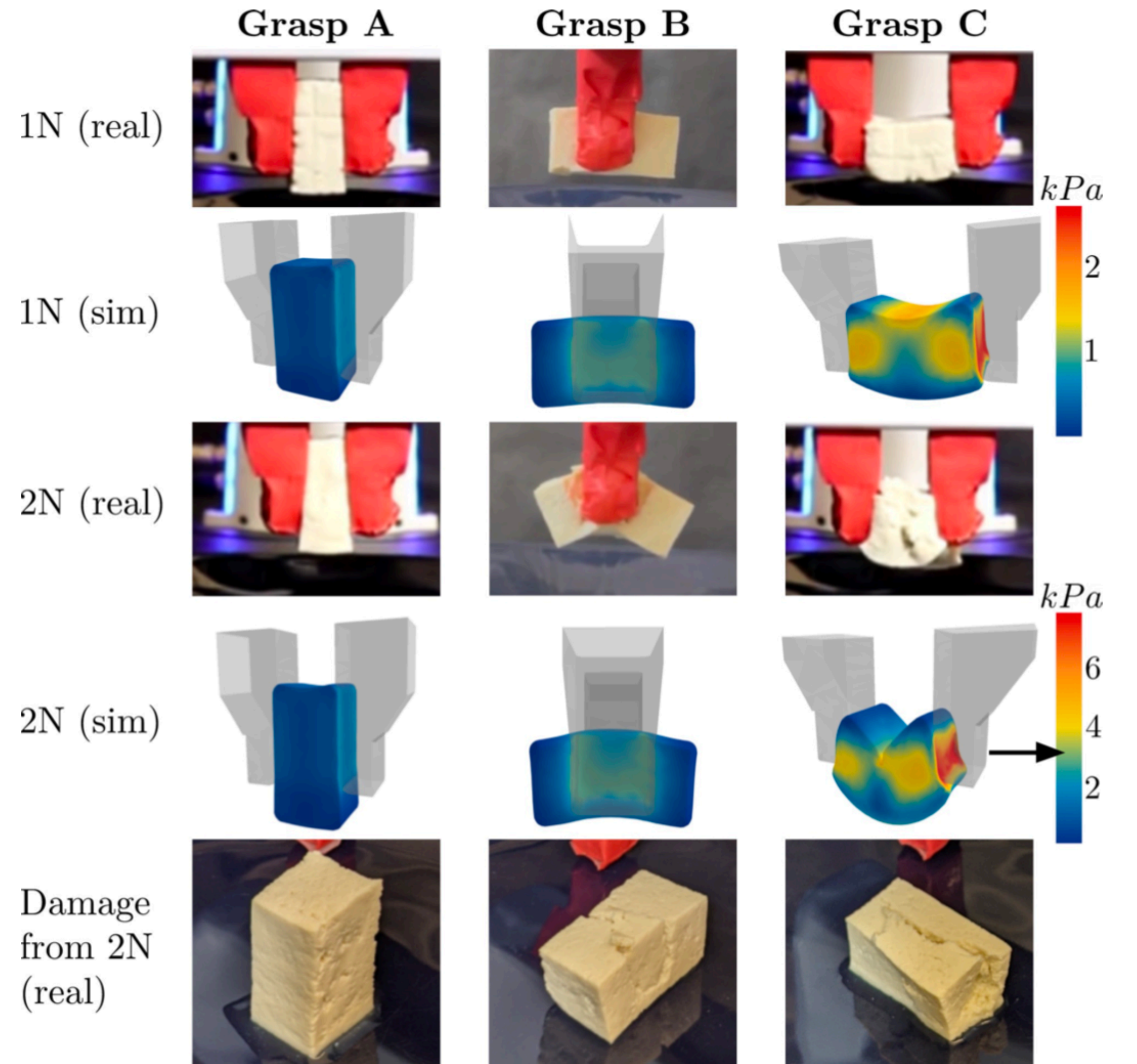


Fig. 9: Three grasps tested on blocks of tofu (1 and 2 N of squeezing force) show similar outcomes in simulation and the real world. Real areas of fracture correspond to simulated stress greater than 3 kPa , the estimated breaking stress (denoted on color bar by black arrow).

Sim2Real Latex Tubes

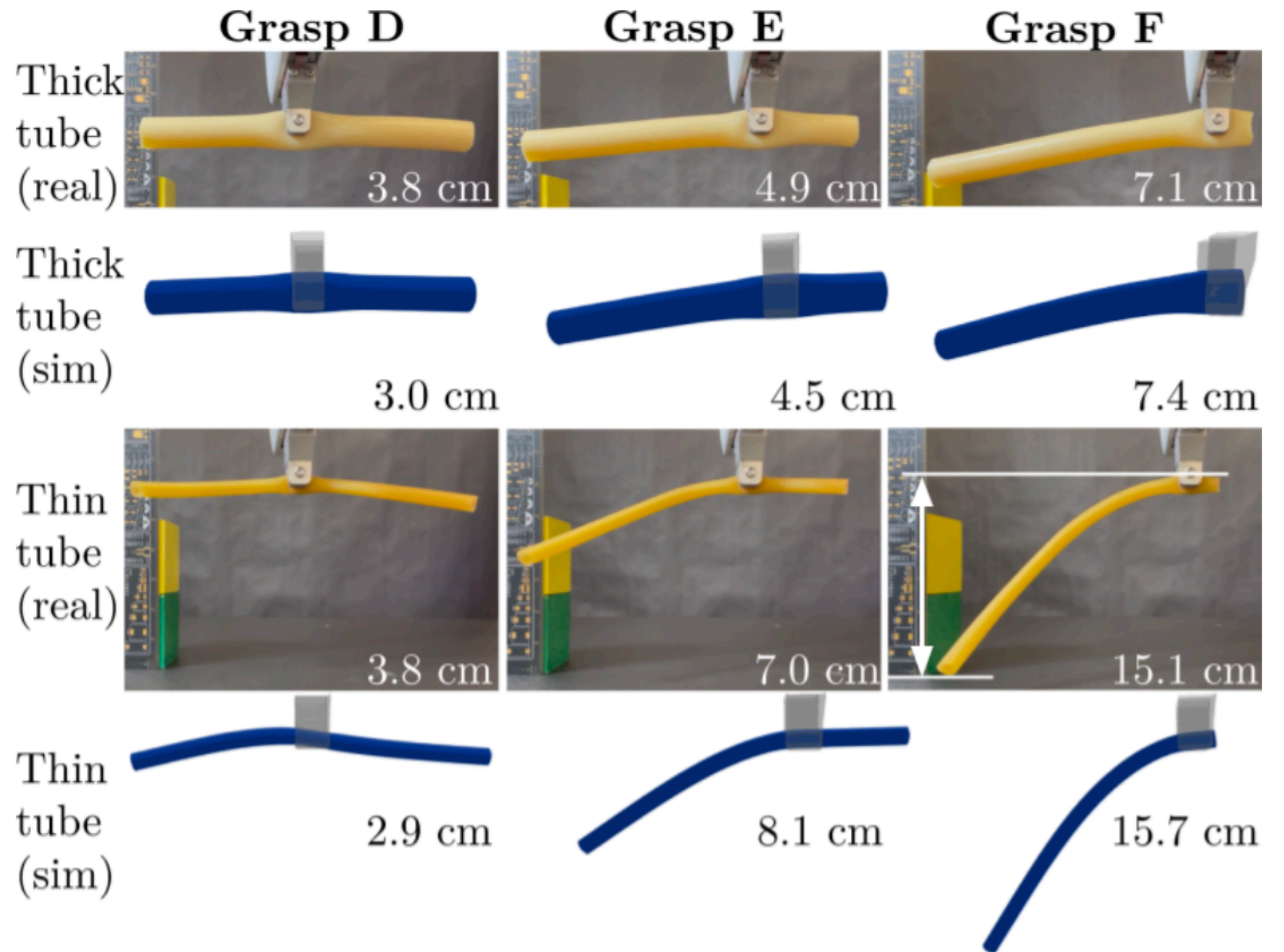
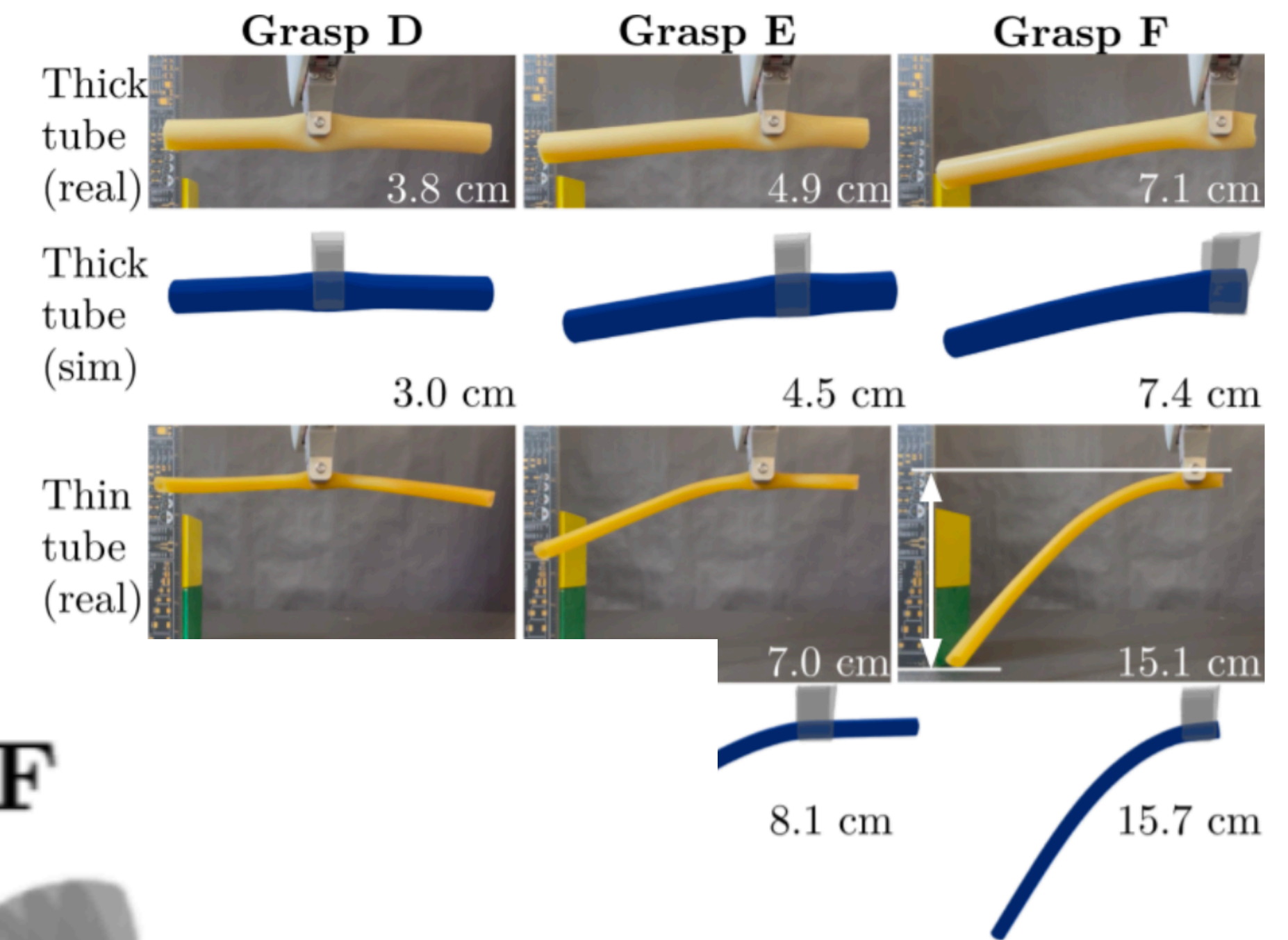


Fig. 10: Three grasps tested on 2 real and simulated latex tubes under 15 N of gripper force. The vertical distance between the highest and lowest points of the tube is annotated. Localized deformation due to compression at the grippers is replicated in simulation.

Sim2Real Latex Tubes



and simulated latex tubes under
stance between the highest and
. Localized deformation due to
ted in simulation.

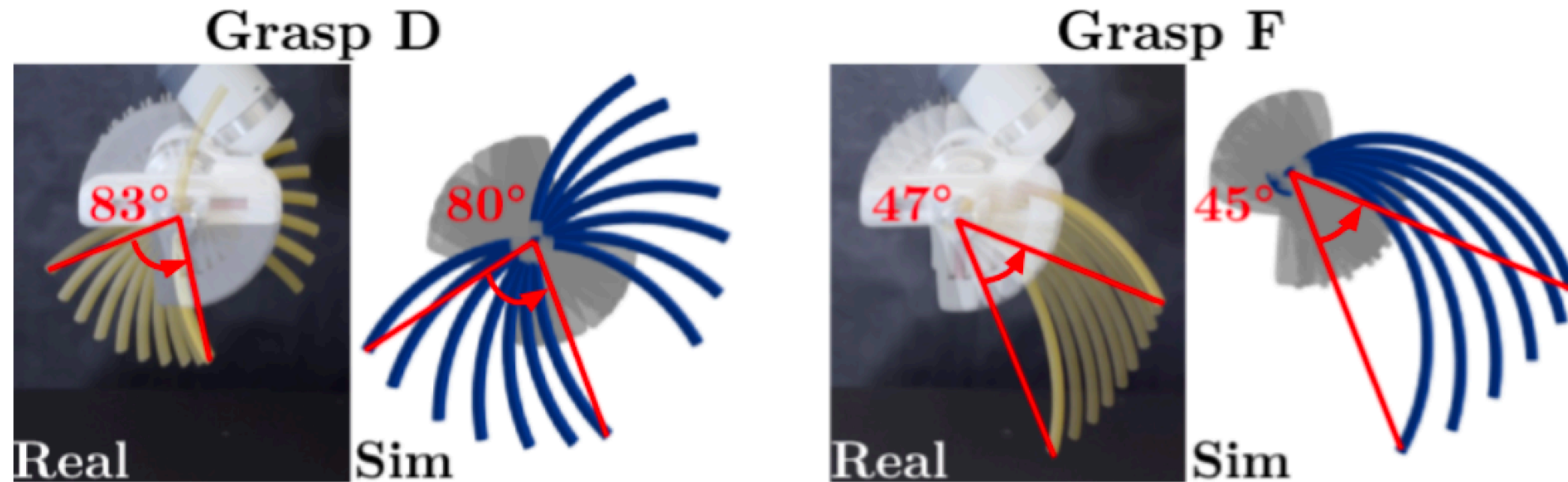


Fig. 11: A middle grasp (grasp D) and end grasp (grasp F) under a counterclockwise 90° rotation of the gripper in the real world and in simulation. The angles swept out by the tube tip are marked in red.

Sim2Real Bleach Bottle



Grasp G

Grasp H

Grasp I

Grasp J

Grasp K

Fig. 12: Five tested grasps on a real bleach bottle. Grasps are also repeated in simulation.



Fig. 12: Five tested grasps on a rea repeated in simulation.

Sim2Real Bleach Bottle

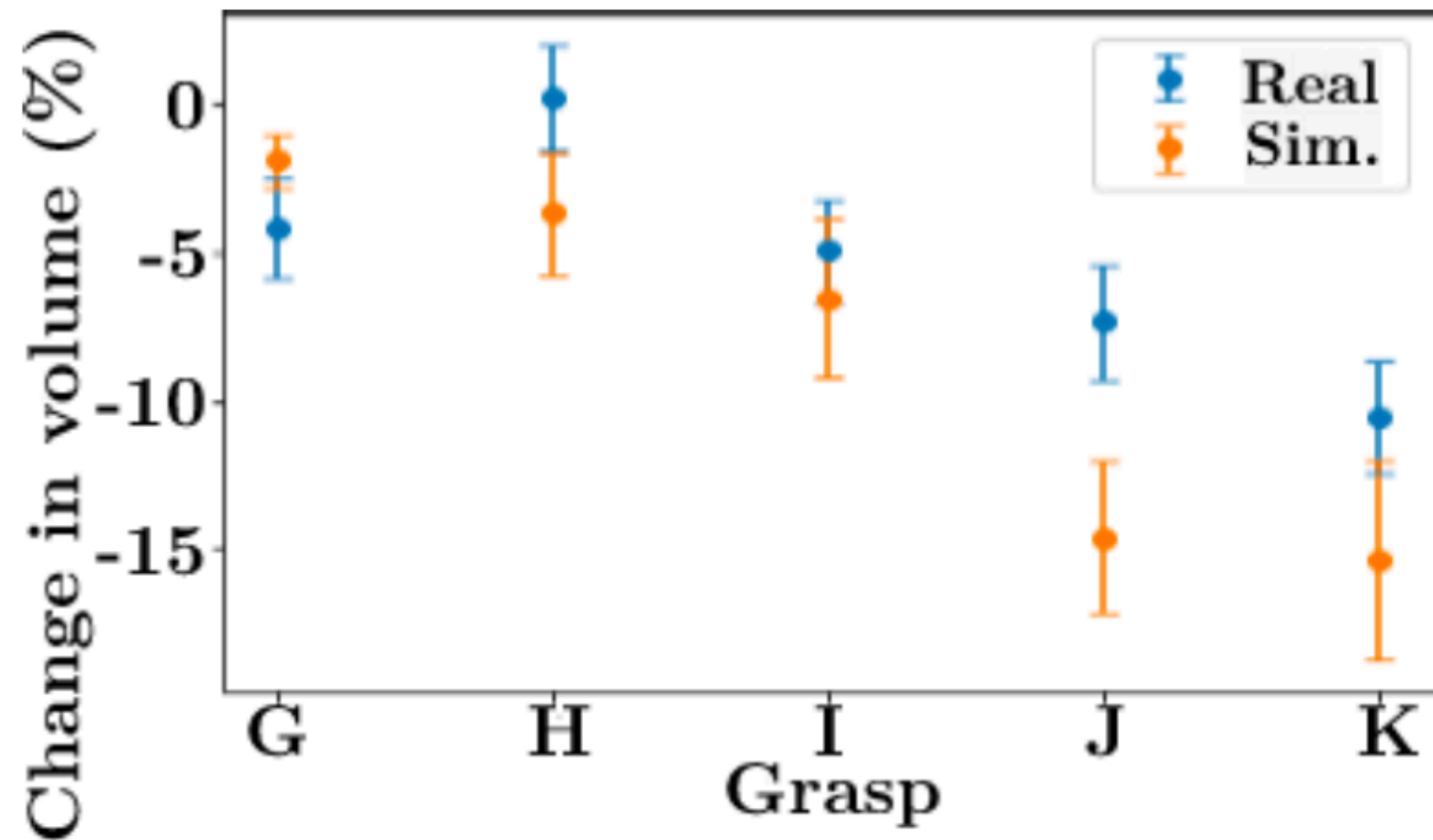


Fig. 13: Percent volume change pre- and post-grasp for the real and simulated bleach bottles under grasps G to K.

Sim2Real Plastic Cup

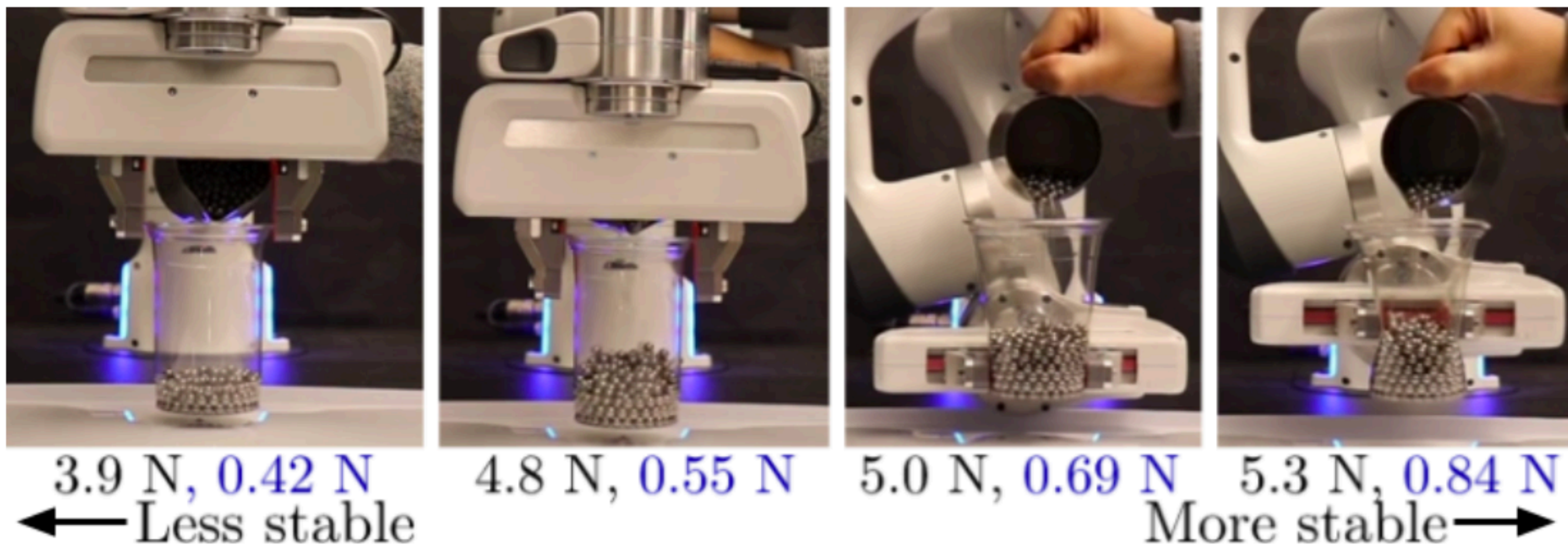
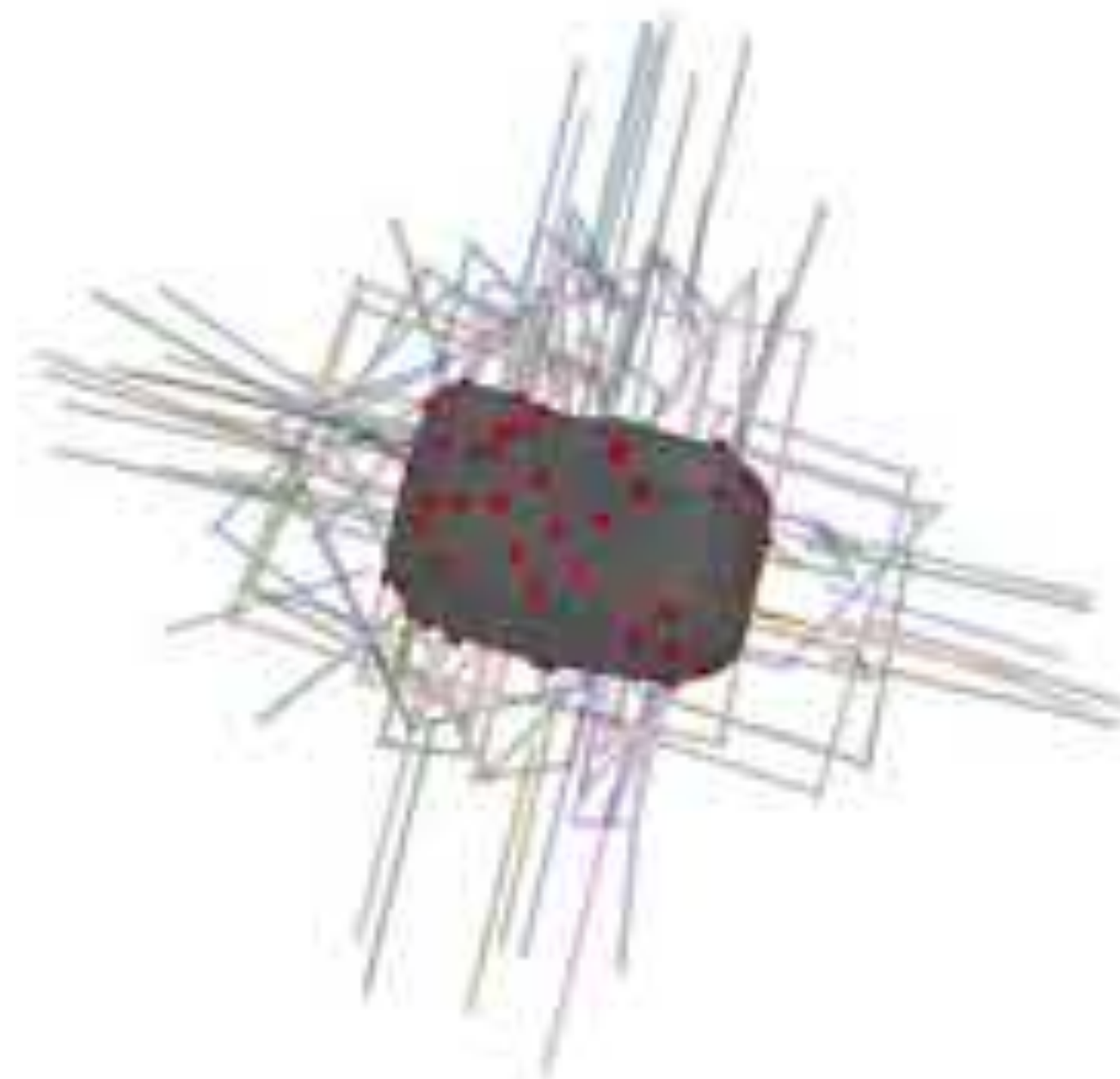


Fig. 14: Under four grasps on a plastic cup, the maximum weight withstood before loss of contact is annotated for both the real world (black) and in simulation (blue).

Suggested Applications

1. Learning representations of new high-dimensional features and metrics (e.g., for object and contact geometry, field quantities, etc.) for memory-efficient grasp planning
2. Customizing grasping experiments to create task-oriented planners (e.g., to minimize food deformation)
3. Performing rigorous, direct comparisons between simulation and reality on custom deformables of interest (e.g., on organs for robotic surgery)
4. Generating training data for real-world system identification (e.g., tactile probing on unknown materials)
5. Generating data for neural network-based grasp simulation for real-time grasp planning
6. Improving grasp planning robustness to uncertainty in object material properties (e.g., via domain randomization)

1. 2:27
2. 12:26



DefGraspSim: Simulation-based grasping of 3D deformable objects

Isabella Huang, Yashraj Narang, Clemens Eppner, Balakumar Sundaralingam, Miles Macklin, Tucker Hermans, Dieter Fox

Overview

This website contains the following supplementary information for our submission:

1. Additional **videos** of simulated and real experiments
2. The **codebase** developed for our simulations, which can be used to simulate and evaluate grasps on arbitrary 3D deformable objects
3. The **datasets** containing measured grasp features and performance metrics on object primitives and complex objects
4. **Interactive visualizations** of grasp results on object primitives

<https://sites.google.com/nvidia.com/defgraspsim>

IPC-GraspSim: Reducing the Sim2Real Gap for Parallel-Jaw Grasping with the Incremental Potential Contact Model

Chung Min Kim¹, Michael Danielczuk¹, Isabella Huang², Ken Goldberg¹

Abstract—Accurately simulating whether an object will be lifted securely or dropped during grasping is a longstanding Sim2Real challenge. Soft compliant jaw tips are almost universally used with parallel-jaw robot grippers due to their ability to increase contact area and friction between the jaws and the object to be manipulated. However, interactions between the compliant surfaces and rigid objects are notoriously difficult to model. We introduce IPC-GraspSim, a novel grasp simulator that extends Incremental Potential Contact (IPC) — a highly accurate collision + deformation model developed in 2020 for computer graphics. IPC-GraspSim models both the dynamics and the deformation of compliant jaw tips to reduce Sim2Real gap for robot grasping. We evaluate IPC-GraspSim using a set of 2,000 physical grasps across 16 adversarial objects where analytic models perform poorly. In comparison to both analytic quasistatic contact models (soft point contact, REACH, 6DFC) and dynamic grasp simulators (Isaac Gym with FleX), results suggest IPC-GraspSim can predict robustness with higher precision and recall ($F1 = 0.85$). IPC-GraspSim increases F1 score by 0.03 to 0.20 over analytic baselines and 0.09 over Isaac Gym, at a cost of 8000x and 1.5x more compute time, respectively. All data, code, videos, and supplementary material are available at <https://sites.google.com/berkeley.edu/ipcgraspsim>.

Positive:
Sim predicts success
Real grasp succeeds

True Negative:
Sim predicts failure
Real grasp fails

False Positive:
Sim predicts success
Real grasp fails

False Negative:
Sim predicts failure
Real grasp succeeds

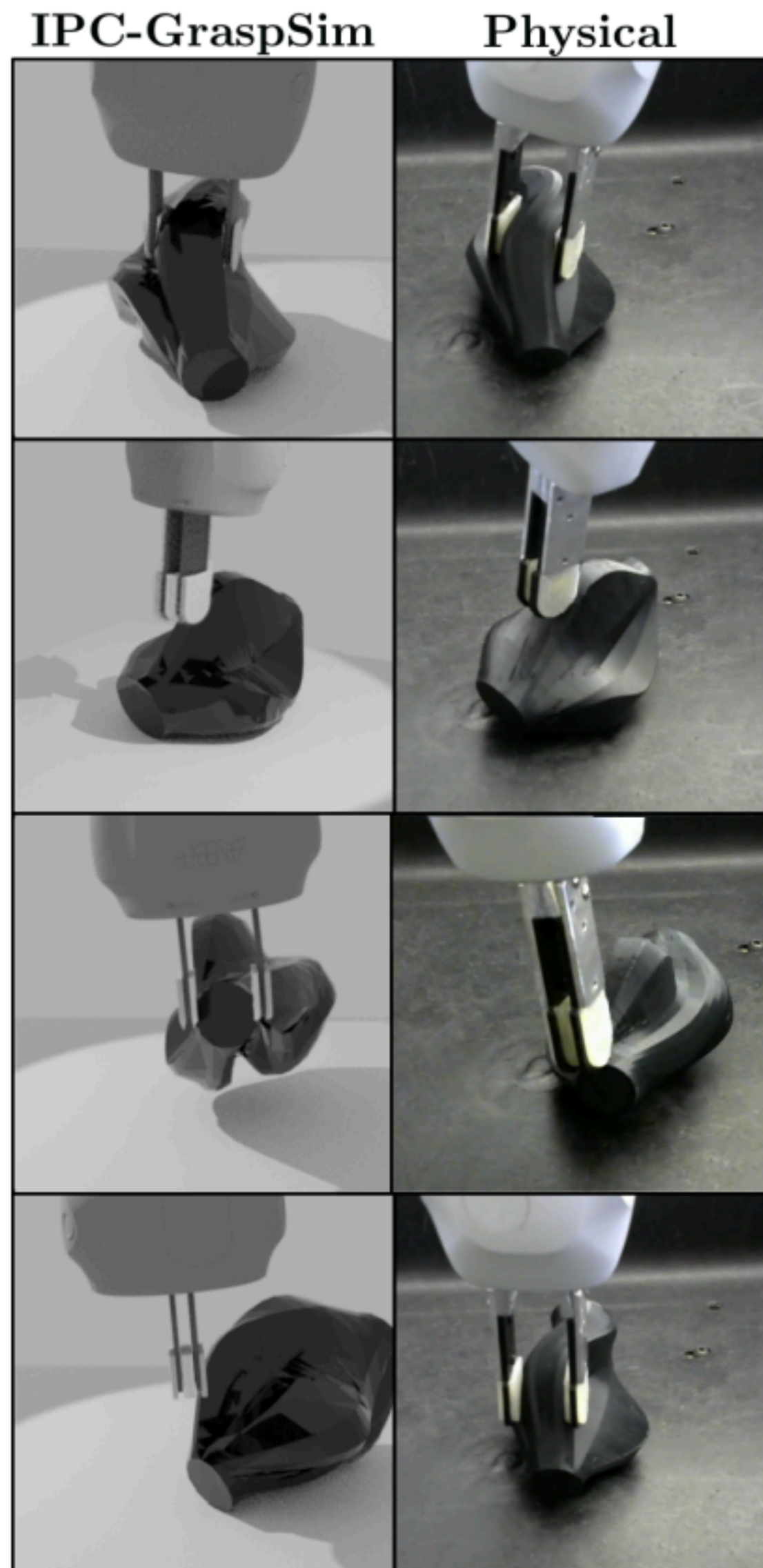
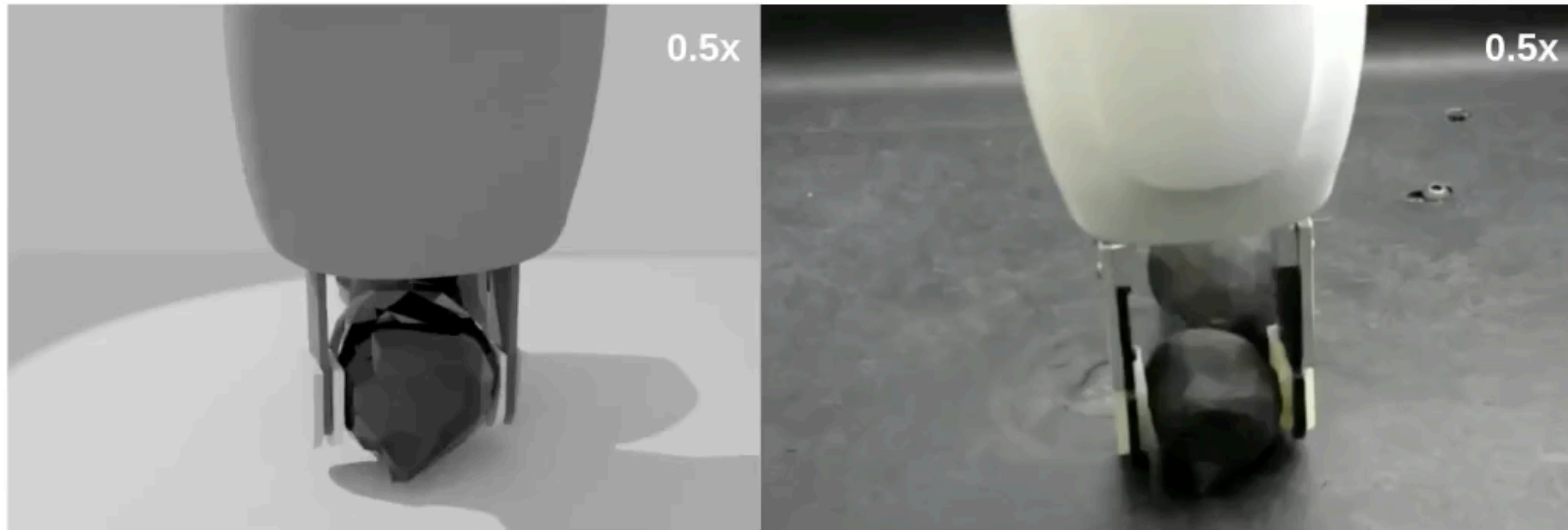


Fig. 1: Simulated (left) and physical (right) grasp outcomes: in the first two rows, IPC-GraspSim correctly predicts grasp success and grasp failure. In the last two rows, predictions are incorrect due to unmodeled cantilever bending + rotations due to pushing.

Simulation of Parallel-Jaw Grasping using Incremental Potential Contact Models

Chung Min Kim, Michael Danielczuk, Isabella Huang, Ken Goldberg



Berkeley
UNIVERSITY OF CALIFORNIA

AUTOLAB

 **BAIR**
BERKELEY ARTIFICIAL INTELLIGENCE RESEARCH

<https://sites.google.com/berkeley.edu/ipcgraspsim>

Bimanual Handling of Deformable Objects With Hybrid Adhesion

Amy Kyungwon Han ^{id}, Amar Hajj-Ahmad ^{id}, and Mark R. Cutkosky ^{id}

Abstract—We present hybrid adhesive end-effectors for bimanual handling of deformable objects. The gripping system is driven by the need to achieve alignment on deformable and irregular surfaces while maintaining a large area of contact for efficient use of the adhesive. The objective of the gripping system is to reduce the internal grasping force needed to securely lift and manipulate objects with two arms, for example, in warehousing and retail environments. The end-effectors are designed with features meant to accommodate surface irregularities in macroscale form, mesoscale waviness, and microscale roughness, achieving good shear adhesion on surfaces with little gripping force. The new gripping system combines passive mechanical compliance with a hybrid electrostatic-adhesive pad so that humanoid robots can grasp a wide range of materials including paperboard and textured plastics with internal grasping forces of 1 N and 0.5 N, respectively. These grasping forces are more than 10 times smaller than without the hybrid pad. As an application, we demonstrate a humanoid robot handling delicate deformable objects ranging from flowers in a plastic sleeve to a 2.4 kg sack of rice with less than 1.5 N of normal gripping force.

Index Terms—Bimanual manipulation, biomimetics, grippers and other end-effectors, mechanism design.

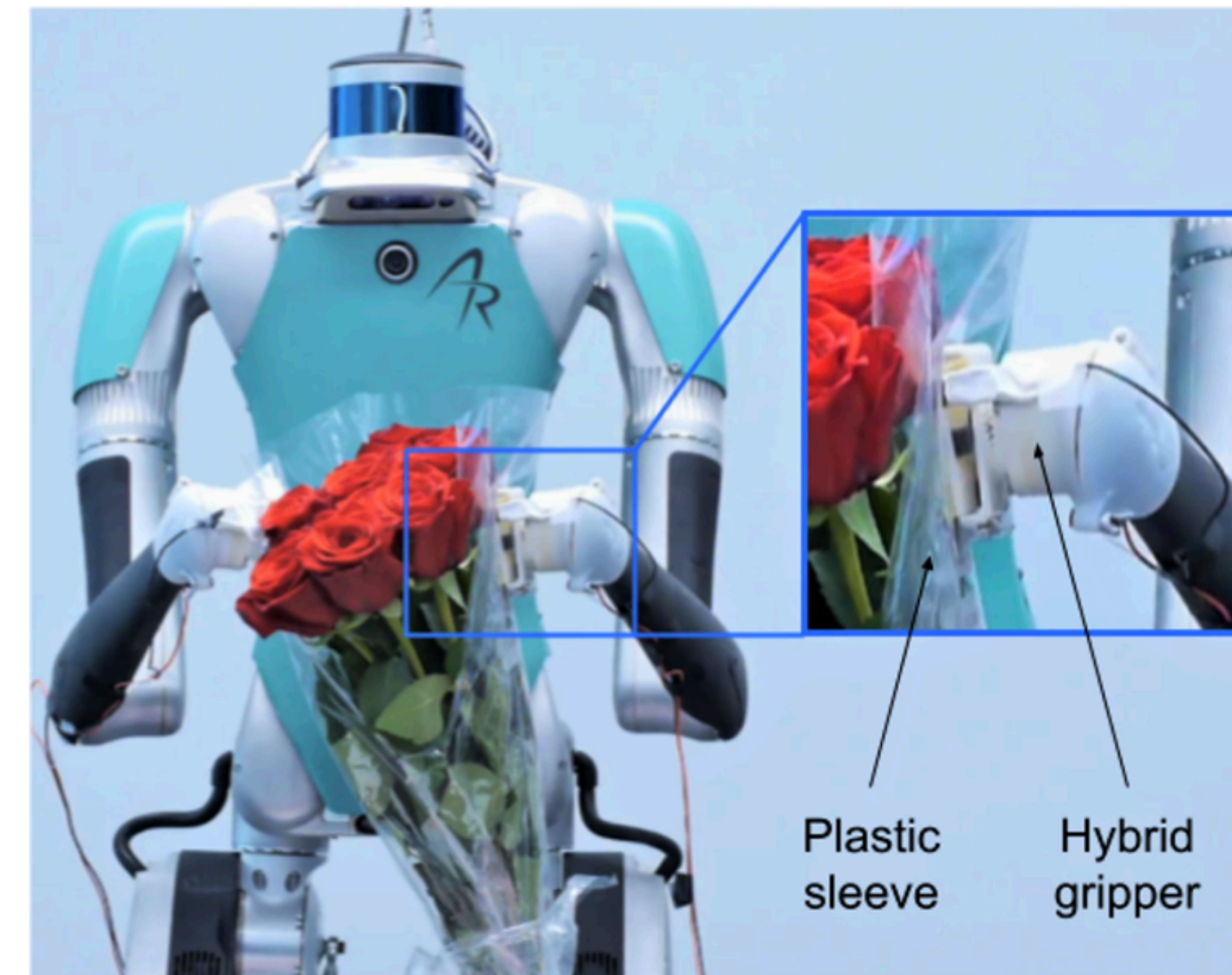


Fig. 1. A bimanual mobile robot lifting a delicate flower bouquet with hybrid adhesive gripper.

Bimanual Handling of Deformable Objects with Hybrid Adhesion

Amy Kyungwon Han^{*[1] [2]}, Amar Hajj-Ahmad^{*[1]}, and Mark R. Cutkosky^[1]

^[1] Department of Mechanical Engineering, Stanford University, Stanford, CA 94305, USA

^[2] Department of Mechanical Engineering, Seoul National University, Seoul 08826, Korea



Virtual Reality Based Tactile Sensing Enhancements for Bilateral Teleoperation System with In-Hand Manipulation

Yi Liu^{1,*}, Ya-Yen Tsai^{2,*}, Bidan Huang^{3†} and Jing Guo¹

Abstract—Tactile sensing is important for contact-rich tasks especially in where an in-hand manipulation is involved. In teleoperation, such feedback can provide information of when and where the contacts happen, and is essential for a human operator to make appropriate actions. To improve the experience in human-robot interaction in teleoperation without vision feedback, in this paper, a model-based sensing enhancement system is proposed. This system allows a human operator to remotely control a dexterous robotics hand with a contact feedback in the form of haptics. Under this framework, we introduce a calibration method to map the hand joint movements of the master and the slave. Given noisy robot sensory data, a learning based approach is adopted to estimate the object pose online. The estimated pose is sent to Unity, of which is leveraged to calculate the hand-object contact force. Finally, this force is rendered to the master, a wearable haptic device, worn by the operator. Our experiments have shown that with this contact information, the performance surpassed those conducted on a bilateral teleoperation system without sense of contact. Additionally, the user can safely manipulate the object with the robot’s hand.

Index Terms—Humanoid robot systems, haptics and haptic interfaces, virtual reality and interfaces.

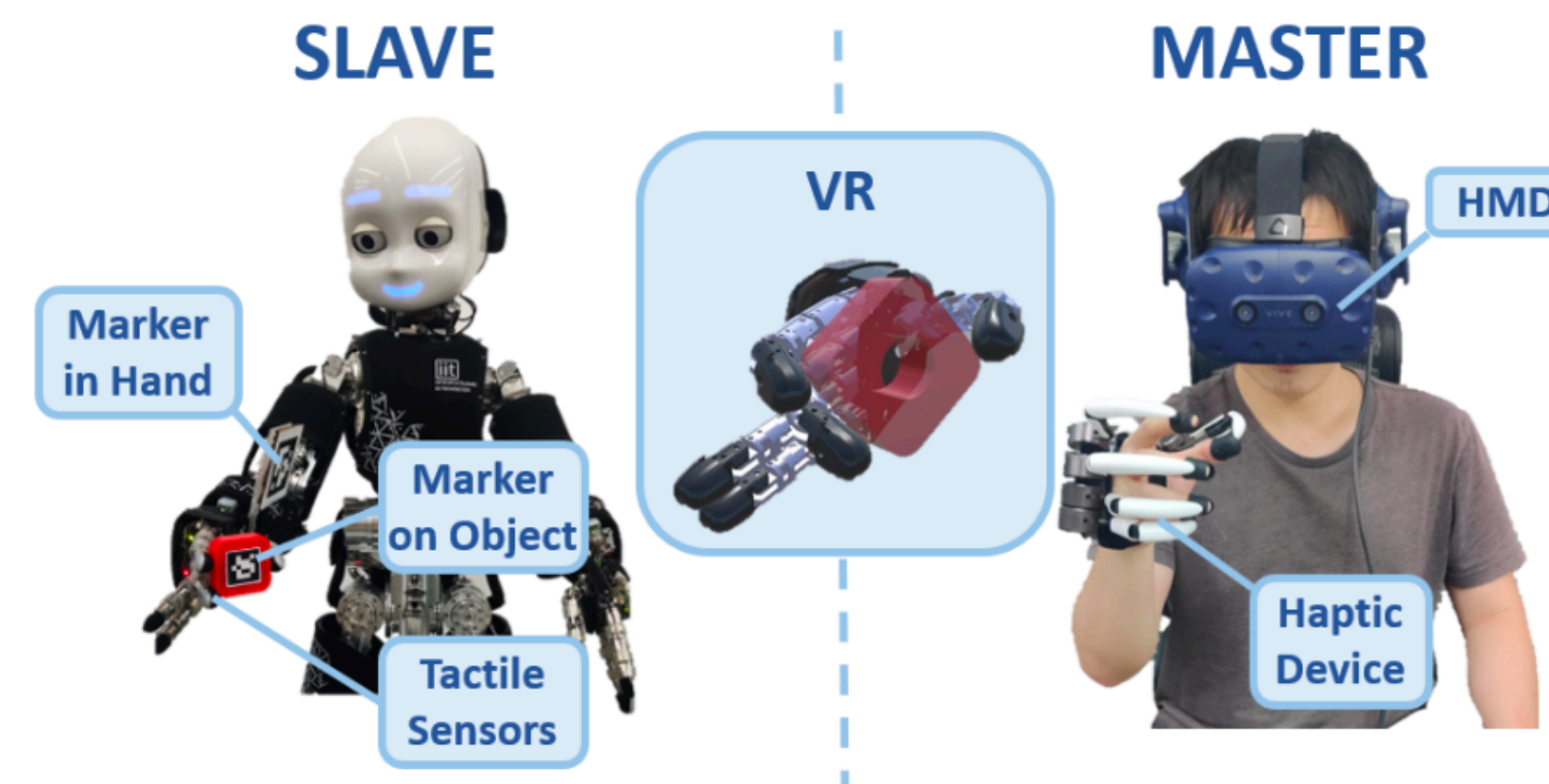


Fig. 1: The system setup consists of the *iCub* robot on the slave side and the human operator wearing a haptic device and a head mounted display (HMD) on the master side. During training, visual markers are attached to the object and the hand for pose tracking. At test time, the vision tracking is replaced by a tactile based tracking method and the simulated force in Unity is rendered on the haptic device.

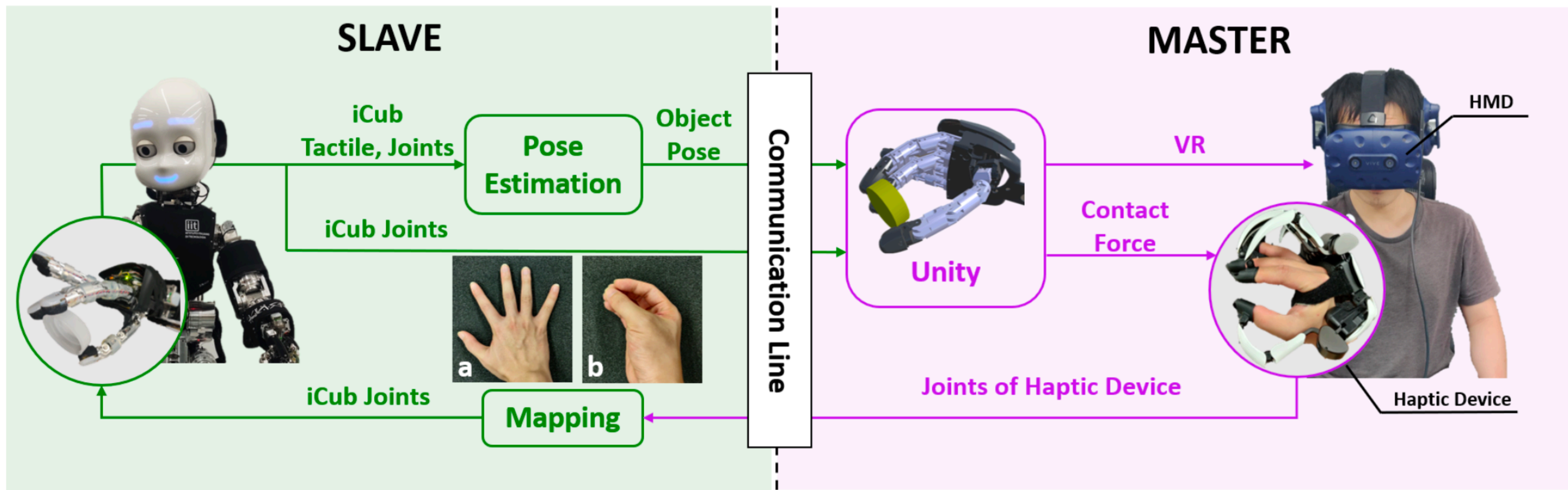


Fig. 2: Overview of the bilateral teleoperation system. Above mapping, (a) and (b) show the hand postures for calibrating as detailed in Section II-C1.



Fig. 3: The anthropomorphic haptic device and the *iCub*'s hand. Left: *Dexmo*. $D_1 - D_5$ are the joints for controlling *iCub*. Right: *iCub*. $J_1 - J_{11}$: the controlled joints. J_4, J_7, J_{10} are coupled with J_3, J_6, J_9 respectively. Each fingertip is equipped with 12 tactile sensors ($T_1 - T_{12}$) arranged as shown.

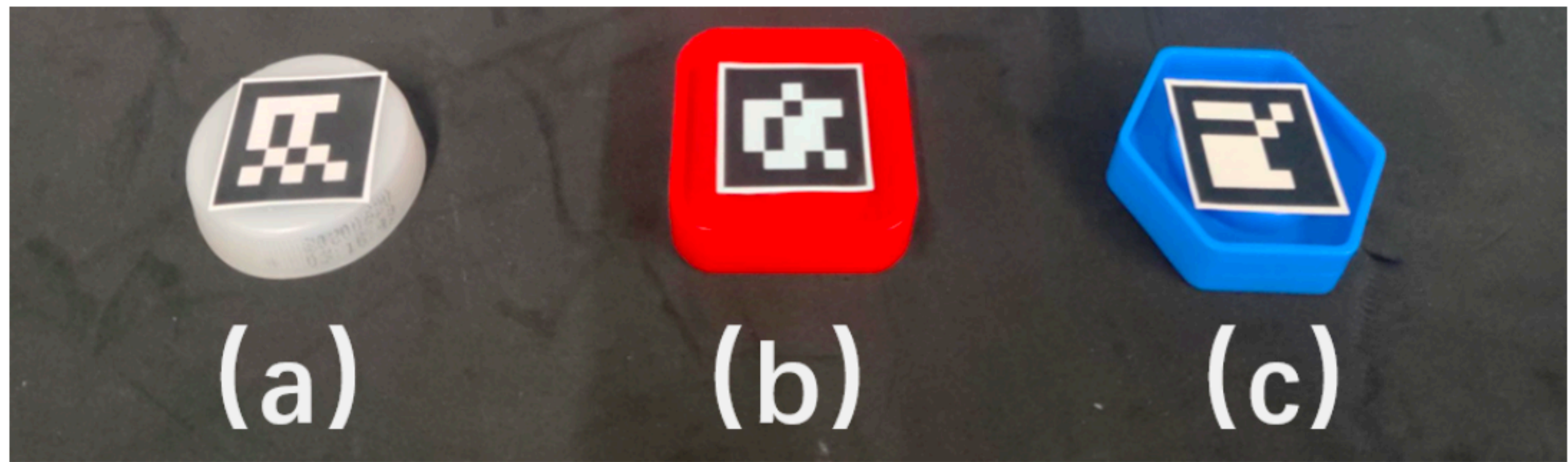
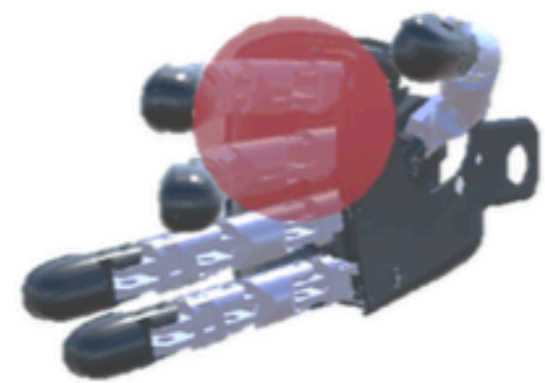
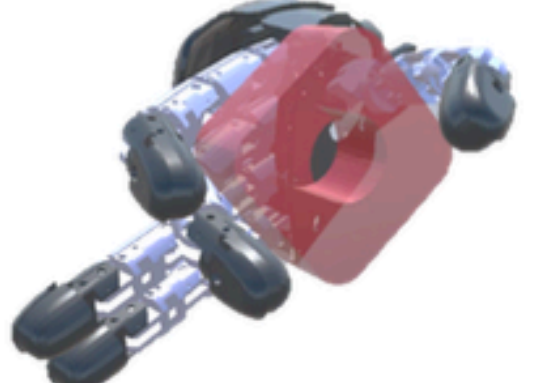



TABLE II: This table shows the pose estimation errors for different objects in hand.

Shape	 Cap	 Square	 Hexagon
Position Error (Mean \pm Std)/(m)	0.0018 \pm 0.0014	0.0017 \pm 0.0037	0.0025 \pm 0.0019
Orientation Error (Mean \pm Std)/(rad)	0.053 \pm 0.094	0.122 \pm 0.222	0.167 \pm 0.207

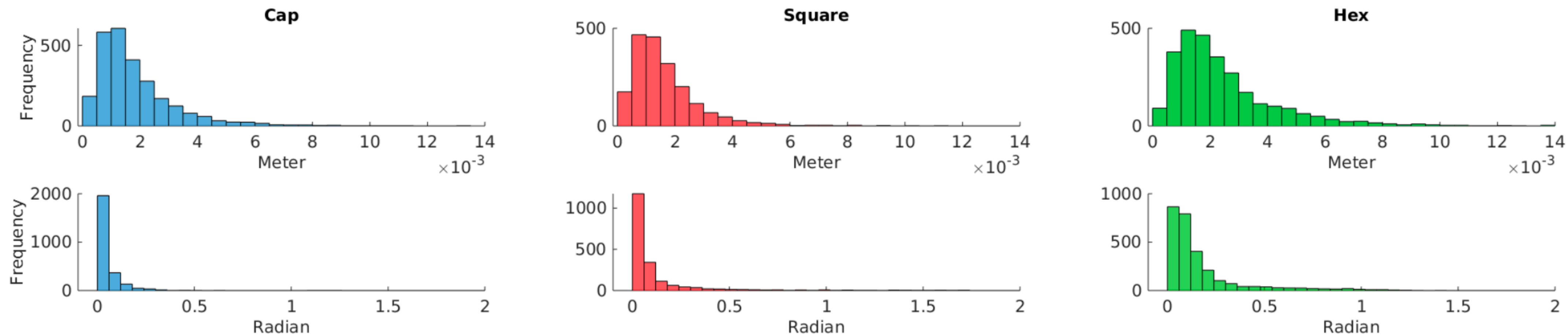


Fig. 6: Histograms of the errors of the pose estimation model. The first row shows the translation and the second row shows the orientation.

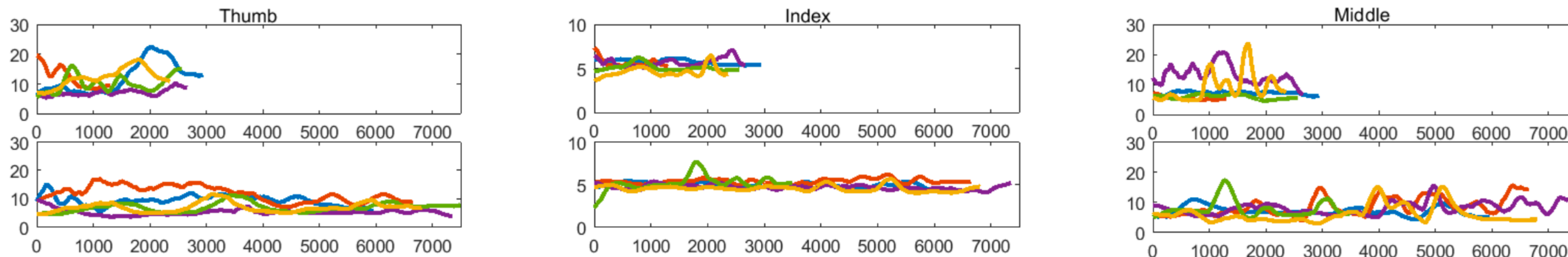


Fig. 7: Tactile sensing comparisons between the proposed (upper) and the standard (lower) teleoperation approaches. Different colors represent different operators. Y-axis represents the sum of tactile signal, X-axis represents the number of steps, based on the frequency of 50Hz.

✓ In the setting of the proposed approach, the tactile and *iCub*'s joints information were taken for the pose estimation of the object. This pose was sent to Unity to update the pose of the modeled object in simulation. The force between the fingers and the object was then calculated in simulation and sent to *Dexmo* for haptic rendering.

In the settings of the standard bilateral teleoperation system, the tactile sensors of *iCub* were directly mapped and rendered to *Dexmo*. Since the tactile signal ranges from 0 to 100, and the torque intensity of the motors in *Dexmo* only ranges from 0 to 1, a linear mapping was done to relate the tactile signal to the motor torque intensity. For each finger, the maximum tactile sensor signal was taken as the intensity for the finger.

TABLE III: The mean (μ) and variance (Σ) of haptic feedback values of different methods, and comparison of efficiency between different methods, which represents the ratio of the number of average steps (AS) for the standard vs. proposed methods.

method		thumb	index	middle	AS	efficiency
<i>proposed</i>	μ	12.85	5.31	11.95	2756	146.4%
	Σ	79.80	7.64	32.22		
<i>standard</i>	μ	15.27	8.06	13.94	6790	100%
	Σ	72.05	8.54	103.06		

Artificial Intelligence Enables Real-Time and Intuitive Control of Prostheses via Nerve Interface

Diu Khue Luu*, Anh Tuan Nguyen*, Ming Jiang, Markus W. Drealan, Jian Xu, Tong Wu, Wing-kin Tam, Wenfeng Zhao, Brian Z. H. Lim, Cynthia K. Overstreet, Qi Zhao, Jonathan Cheng, Edward W. Keefer, Zhi Yang**

IEEE Transactions on
Biomedical Engineering (2022).

Abstract—Objective: The next generation prosthetic hand that moves and feels like a real hand requires a robust neural interconnection between the human minds and machines. ***Methods:*** Here we present a neuroprosthetic system to demonstrate that principle by employing an artificial intelligence (AI) agent to translate the amputee’s movement intent through a peripheral nerve interface. The AI agent is designed based on the recurrent neural network (RNN) and could simultaneously decode six degree-of-freedom (DOF) from multichannel nerve data in real-time. The decoder’s performance is characterized in motor decoding experiments with three human amputees. ***Results:*** First, we show the AI agent enables amputees to intuitively control a prosthetic hand with individual finger and wrist movements up to 97-98% accuracy. Second, we demonstrate the AI agent’s real-time performance by measuring the reaction time and information throughput in a hand gesture matching task. Third, we investigate the AI agent’s long-term uses and show the decoder’s robust predictive performance over a 16-month implant duration. ***Conclusion & significance:*** Our study demonstrates the potential of AI-enabled nerve technology, underling the next generation of dexterous and intuitive prosthetic hands.

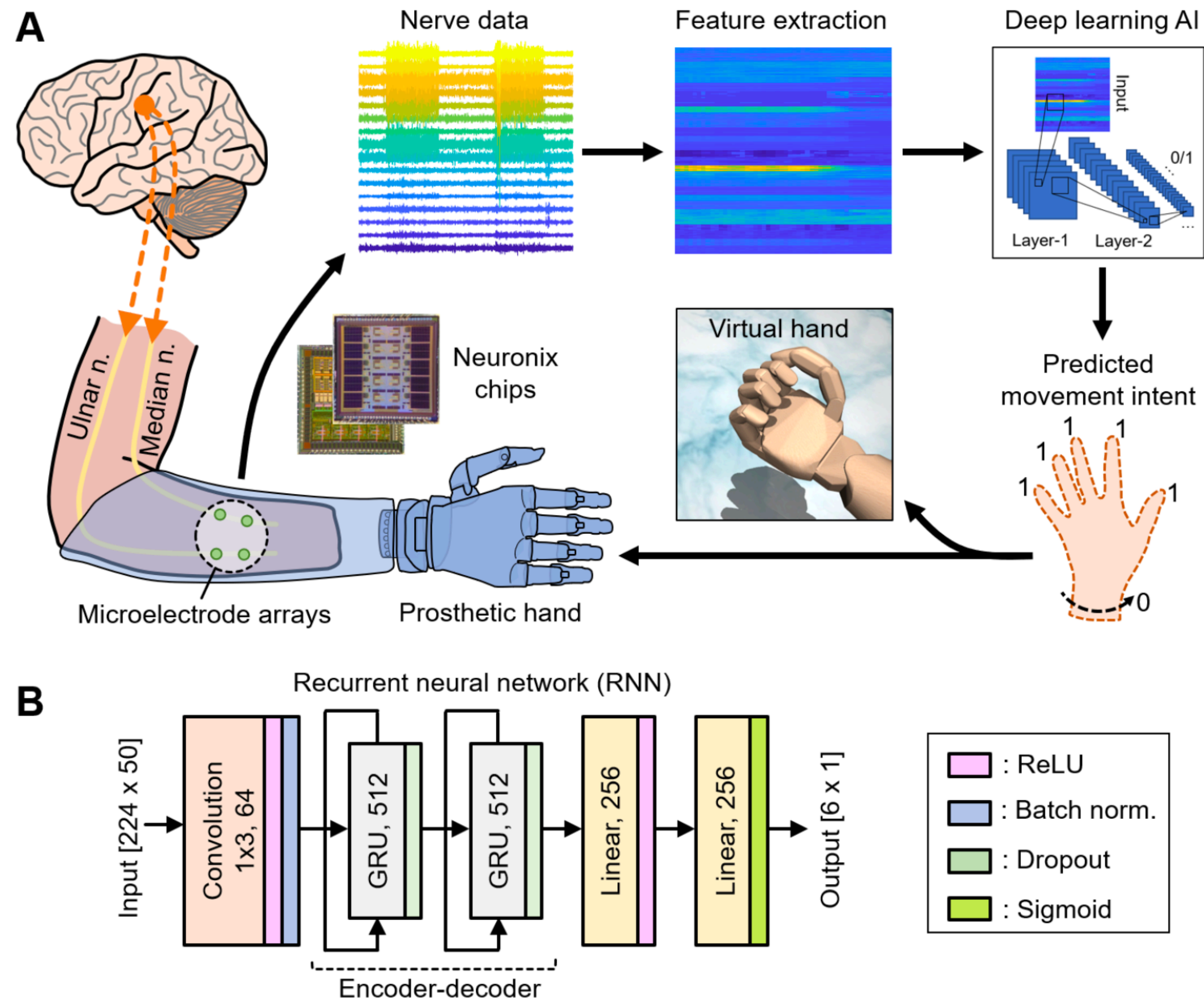


Fig. 1. (A) Overview of the AI neural decoder and signal processing paradigm. Nerve data are acquired from the subject's amputated arm by Neuronix neural interface chips, followed by feature extraction. The deep learning AI then uses feature data to predict the subject's intent of moving several DOF simultaneously. The predictions are mapped to movements of a virtual hand or a prosthetic hand in real-time. (B) Design of the deep learning AI based on the recurrent neural network (RNN) architecture.

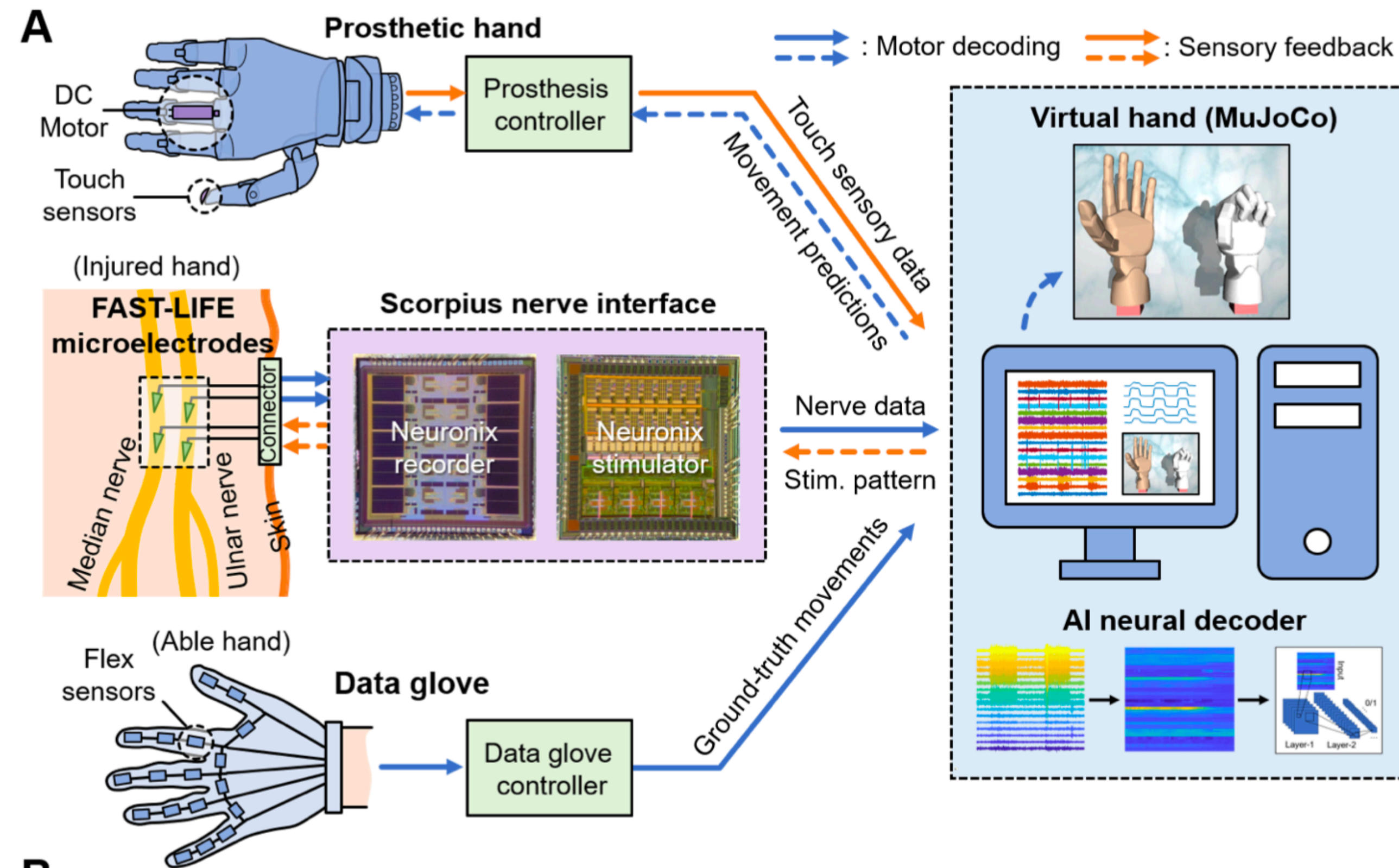


Fig. 2. (A) Overview of the experiment setup with both neural recording and stimulation capabilities. (Blue path) The motor decoding dataset is obtained via a mirrored bilateral paradigm. Nerve data and ground-truth movements are simultaneously acquired from the injured and able hand, respectively. All signal processing, neural decoding, and real-time displaying are done on a desktop PC. Movement predictions can be mapped to a prosthetic hand or a virtual hand. (Orange path) The setup also includes components like touch sensors and neurostimulators for somatosensory restoration as detailed in [40], [41]. (C) Photos of three subjects in an experiment session.

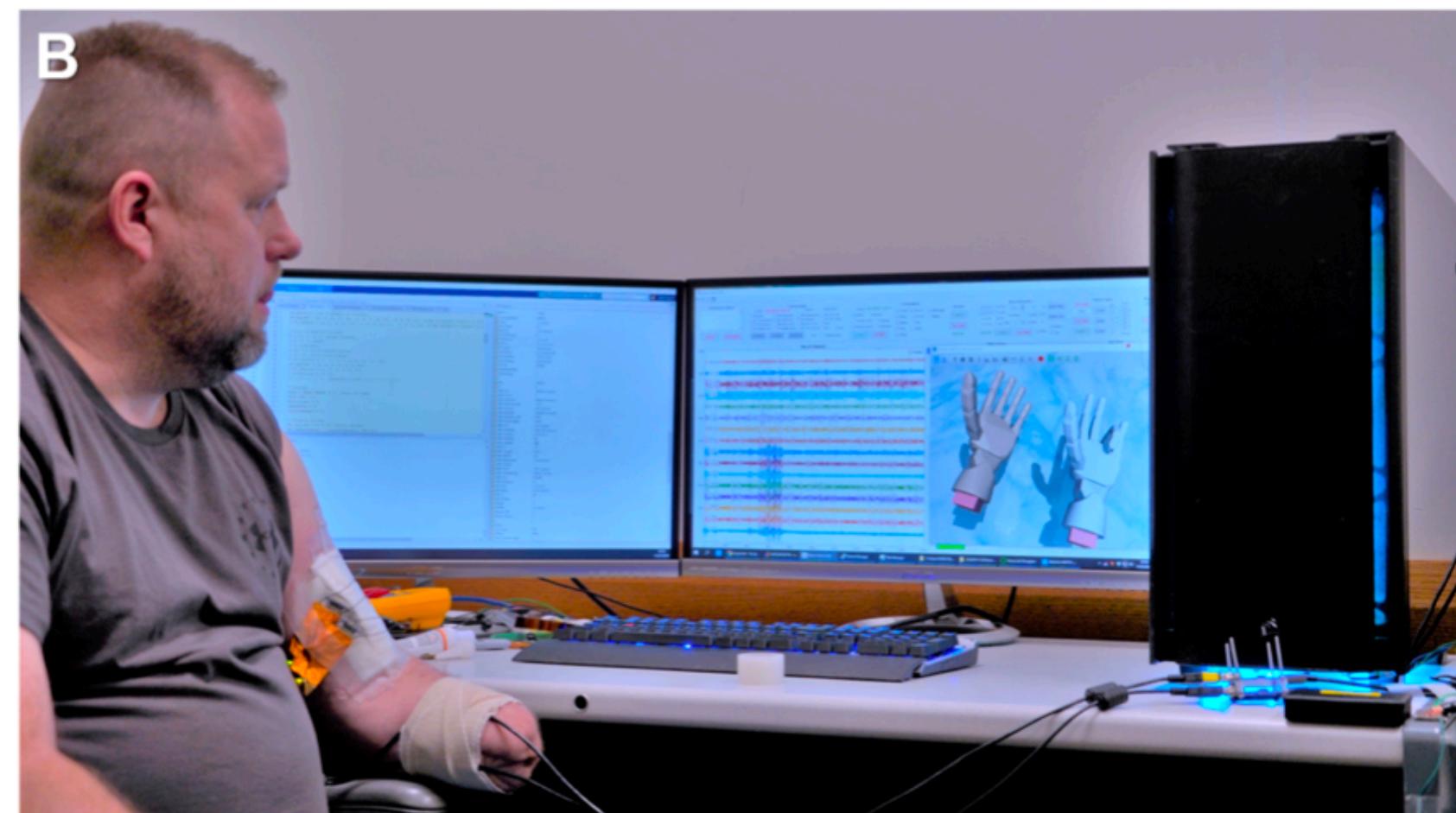
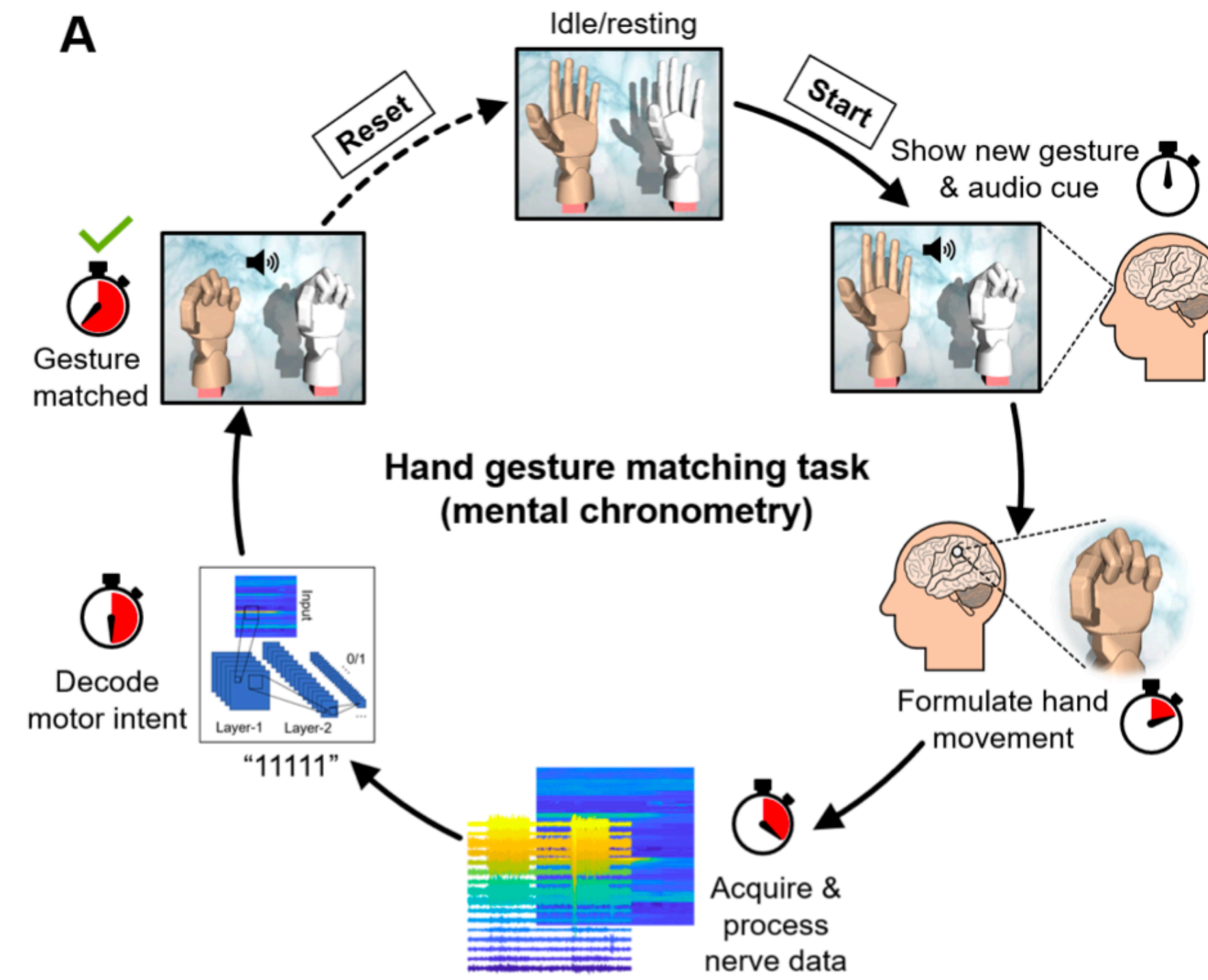


Fig. 3. (A) Schematic of the hand gesture matching task to measure the end-to-end reaction time (mental chronometry) and the information throughput of the entire nerve interface and motor decoding. In each trial, the subject is shown a random hand gesture, which he attempts to match with the AI neural decoder running in real-time. (B) Photo of Subject SF performing the task. Real-time nerve data and current AI's prediction can be seen on the monitor.

TABLE II
SUMMARY OF MOTOR DECODING DATASETS

Subject	No. of channels	Training samples	Testing samples	No. of DOF	No. of gestures*
NB	8	174,782	19,419	5	10
CS	16	112,667	17,525	6	8
SF	16	241,511	20,087	6	11

*Gestures include resting.

TABLE IV
SUMMARY OF PERFORMANCE METRICS OF THE MATCHING TASK

Gesture	Number of trials	Success rate @3 sec (%)	Median reaction time (sec)	Mean reaction Time (sec)	Info. throughput (bps [bpm])
Thumb flex	38	100.0	0.75	0.77	6.67 [400.2]
Index flex	51	100.0	0.77	0.80	6.48 [388.8]
Middle flex	45	100.0	0.76	0.84	6.61 [396.6]
Ring flex	47	100.0	0.92	1.14	5.41 [324.6]
Little flex	42	92.9	0.79	1.00	5.88 [352.8]
Index pinch	37	100.0	1.04	1.05	4.80 [288.0]
Fist/grip	49	100.0	0.83	0.92	6.03 [361.8]
Wrist pronation	48	98.1	0.74	0.84	6.71 [402.6]
All gestures	357	99.2	0.81	0.92	6.09 [365.4]

